Non-peer reviewed preprint submitted to EarthArXiv

Probabilistic modelling of pharmaceutical pollution risk from sewage treatment work discharges using a Bayesian Network: application to a Scottish river catchment

Mads Troldborg[1*], Miriam Glendell[2*], Zisis Gagkas[2], Kerr Adams[2], Camilla Negri[2], Phil Taylor[4], Zulin Zhang[2], Pat Cooper[2], Alison Brown[3], Linda May[4], Ana Corrochano-Fraile[5], Lindsay Beevers[5], Andrew Tyler[3]

[1] The James Hutton Institute, Information and Computational Sciences Department, Invergowrie, Dundee, United Kingdom.
[2] The James Hutton Institute, Environmental and Biochemical Sciences Department, Craigiebuckler, Aberdeen, United Kingdom.
[3] University of Stirling, Stirling, United Kingdom.
[4] UK Centre for Ecology & Hydrology. Bush Estate, Penicuik, Midlothian, United Kingdom.
[5] Institute of Infrastructure and Environment, School of Engineering, University of Edinburgh, Edinburgh, United Kingdom.

* Corresponding authors: mads.troldborg@hutton.ac.uk, miriam.glendell@hutton.ac.uk

Keywords: Pharmaceutical pollution; Bayesian Network; Sewage Treatment Works; Water quality; Risk assessment; Climate Change

ABSTRACT

Pharmaceuticals are increasingly recognised as a class of emerging contaminants of concern in rivers. Their continuous release from human use and variable removal in sewage treatment works (STWs) can produce ecologically relevant concentrations and contribute to antimicrobial resistance. We developed a probabilistic catchment-scale model based on a Bayesian Network (BN) to quantify pharmaceutical concentrations and the probability of exceeding predicted no-effect concentrations at a monthly time step. The BN embeds a stochastic mass-balance linking monthly prescribing rates, excretion fractions, STW removal efficiencies and river discharge to produce posterior distributions of concentrations for 16 pharmaceuticals at 20 monitoring points in a Scottish catchment. Model inputs were derived from Scotland's National Health Service prescribing records, a literature compilation of excretion and removal data, and a calibrated hydrological model of the catchment. Simulated concentration distributions generally agreed with observations made at the 20 locations over a 16-month period and were typically within one order of magnitude for most compounds, indicating satisfactory performance. Highest exceedance probabilities were predicted for azithromycin, diclofenac, ibuprofen and clarithromycin, particularly at heavily impacted sites and during low-flow summer months. Scenario analyses show that future drier summers (UKCP18 RCP8.5) increase exceedance probabilities, and that substantial reductions in prescribing or markedly improved STW removal efficiencies are needed to reduce risks for high-impact compounds. The BN framework transparently captures uncertainty, supports diagnostic inference (to prioritise interventions) and is readily extensible to include additional sources (e.g., Combined Sewer Overflows or septic tanks) and mixture risk assessment.

1. Introduction

Pharmaceuticals are increasingly recognised as a class of emerging contaminants of concern in freshwater ecosystems. After use, many active pharmaceutical ingredients are incompletely metabolised and subsequently excreted into sewage systems, from where they can enter surface waters through discharges from sewage treatment works (STWs). A wide range of pharmaceuticals have been detected in rivers worldwide, often at concentrations capable of causing ecotoxicological effects, and there is growing concern about their contribution to antimicrobial resistance (AMR) development (aus der Beek et al., 2016; Boxall et al., 2012; Umwelt Bundesamt, 2021; Wilkinson et al., 2022). Unlike classical pollutants, pharmaceuticals are diverse in structure and mode of action, may occur as mixtures or "cocktails," and are often continuously released at low concentrations, creating challenges for risk assessment and management (Boxall et al., 2012; Thornber et al., 2022; 2026).

Understanding the sources, pathways, and fate of pharmaceuticals is therefore critical for developing mitigation strategies. While combined sewer overflows (CSOs), septic tanks, or diffuse pathways may contribute to pharmaceutical pollution, STWs are typically considered the dominant point sources in most catchments (Wu et al., 2025). Pharmaceutical fate is controlled by processes that are uncertain and spatially variable, including prescription and consumption patterns, human excretion, removal during wastewater treatment, hydrological dilution capacity, and instream degradation processes (Jagadeesan et al., 2025; Oldenkamp et al., 2018; Verlicchi et al., 2014; Wu et al., 2025). Models that can integrate these diverse datasets and explicitly represent uncertainty are thus required.

Bayesian Networks (BNs) provide a probabilistic modelling framework that is increasingly applied in environmental risk assessment and management (Glendell et al., 2025; Kaikkonen et al., 2021; Moe

et al., 2021). BNs are graphical models that represent systems as networks of nodes (variables) and conditional dependencies (arrows), enabling probabilistic inference under uncertainty (Pearl, 2014; Korb and Nicholson, 2003). Their advantages are threefold. First, they can integrate heterogeneous and disparate sources of information, including empirical data, literature values, expert knowledge and existing mechanistic model outputs, within a unified framework (Moe et al., 2021; Kaikkonen et al., 2021; Welch et al., 2024). Second, they provide an intuitive, transparent structure that facilitates communication with stakeholders and decision-makers (Adams et al., 2023; Pham et al., 2021). Third, they allow for both predictive inference (e.g. forward propagation of uncertainty from inputs through to outcomes) and diagnostic inference (e.g. backward propagation to identify which variables most influence observed outcomes) (Pearl, 2014; Korb and Nicholson, 2003). This latter capability is particularly useful for scenario analysis (e.g. for identifying which management interventions are most effective) and risk forecasting (e.g. under future climate change). In this sense, BNs go beyond stochastic simulators, offering a platform that can be readily extended to more complex representations of pharmaceutical fate and management scenarios. Several studies have used BNs for modelling water quality in aquatic systems (e.g., Glendell et al., 2022; Troldborg et al., 2021; Welch et al., 2024), however their application to catchment-scale pharmaceutical risk assessments remains novel (Niemi et al., 2024).

The aim of this study is to develop and apply a BN model to quantify the risk of pharmaceutical pollution from STWs within a Scottish river catchment. Specific objectives are to: (i) simulate spatial and temporal concentration patterns and risks of sixteen pharmaceuticals; (ii) evaluate the simulated concentration distributions against field monitoring data to infer key processes controlling risk; and (iii) explore the potential impacts of climate change and management interventions on the probability of exceeding predicted no-effect concentrations. By adopting a BN approach, we demonstrate how a relatively simple mass balance model can be embedded within a flexible probabilistic framework that explicitly represents uncertainties and supports scenario analysis.

2. Methods

2.1 General modelling approach

The modelling framework links prescribed pharmaceutical use to predicted river concentrations and ecological risks through a probabilistic mass balance approach. For each sewage treatment work (STW) *i* in the catchment, the discharged mass load of pharmaceutical *p* to the river was calculated as:

$$L_{p,i} = M_P \times PE_i \times ER_P \times \left(1 - RR_{p,i}\right) \qquad (1)$$

where $L_{p,i}$ [g month^{-1}] is the monthly load of pharmaceutical *p* from the ith STW to the river, M_p [g month^{-1} person^{-1}] is the monthly standardised prescribed mass of pharmaceutical *p*, PE_i [person] is the people equivalent served by the ith STW, ER_p [-] is the fraction of the parent pharmaceutical that is being excreted, and $RR_{p,i}$ [-] is the removal efficiency of pharmaceutical *p* during wastewater treatment at STW *i*.

Thus, M_p x PE_i × ER_p represents the influent load entering the STW, and the factor $(1-RR_{p,i})$ gives the fraction released to the effluent.

At each monitoring point *j* in the river, the concentration of pharmaceutical *p* was then estimated as the sum of upstream loads divided by mean monthly river discharge at the monitoring point Q_j [m^3 month^{-1}]:

$$C_{p,j} = \frac{1}{Q_j} \sum_{i \in U(j)} L_{p,i} \quad (2)$$

where *U(j)* denotes the set of STWs located upstream of monitoring point *j*.

Although the above equations can be solved deterministically, all key parameters (M_p_ER_p, $RR_{p,i}$, Q_j) are subject to uncertainty and variability. To capture this, we implemented the mass balance within a Bayesian Network (BN). Each input parameter is therefore defined by a prior probability distribution (derived from available data, or literature review), and the BN then propagates these uncertainties through to probabilistic predictions (posterior simulations) of concentrations. These concentrations are compared to predicted no-effect concentrations (PNECs) to estimate the probability of ecological risk at each MP and month. This is done by calculating a probabilistic log risk ratio (PLRR) for each pharmaceutical *p* and monitoring point *j* as:

$$PLRR_{P,j} = \log\left(\frac{C_{P,j}}{PNEC_p}\right) \quad (3)$$

The ecological risk is then quantified as the probability that PLRR exceeds zero, i.e. $Pr(PLRR_{p,j} > 0)$, which represents the probability that the pharmaceutical concentration exceeds its PNEC at monitoring point *j* during a given month. This probabilistic formulation allows uncertainty in all upstream processes to be explicitly accounted for in the risk estimate. In the BN implementation, a dedicated node evaluates the probability of PNEC exceedance by discretising the PLRR distribution into values above and below zero.

In order to model the combined load from multiple STWs on the same MP within a single BN, rather than summing the impact from the individual STWs (as in Eq. 2), we specify probability distributions for "catchment effective" input parameters, representing the combined effect of all the STWs within the sub-catchment of the given MP. This means we approximate Eq. 2 as:

$$C_{P,j} = \frac{M_P * PE_{tot} * ER_p * \left(1 - RR_{ef,p}\right)}{Q_j} \quad (4)$$

where PE_{tot} is the total PE served by all STWs in the sub-catchment, and $RR_{ef,p}$ is the effective removal rate given by:

$$RR_{ef,p} = \sum_{i \in U(j)} \frac{PE_i}{PE_{tot}} RR_{p,i} \quad (5)$$

The above effective parameters can all be calculated externally to the BN and used as inputs to the BN model. In the BN implementation, the calculation of the pharmaceutical load $L_{p,i}$ was decomposed into two intermediate steps (Influent load and Effluent load) to visualise how mass is progressively reduced from source to discharge, and to simplify node dependencies. These steps correspond directly to the terms in Eq. (4) above.

The full description of all BN nodes and their parameterisation are given in Supporting information (Table S1.1). The BN for modelling pharmaceutical concentrations and risks of exceeding PNEC at a given monitoring point in a river is shown in Figure 1. It was constructed in *GeNIe* 4.1 (BayesFusion, 2025a) and linked to *R* via the *rSMILE* interface (version 2.4.0) (BayesFusion, 2025b), enabling automated runs for multiple monitoring points and scenarios. A similar technique for linking GeNIe and R was used in Negri et al. (2024) and Niemi et al. (2024).

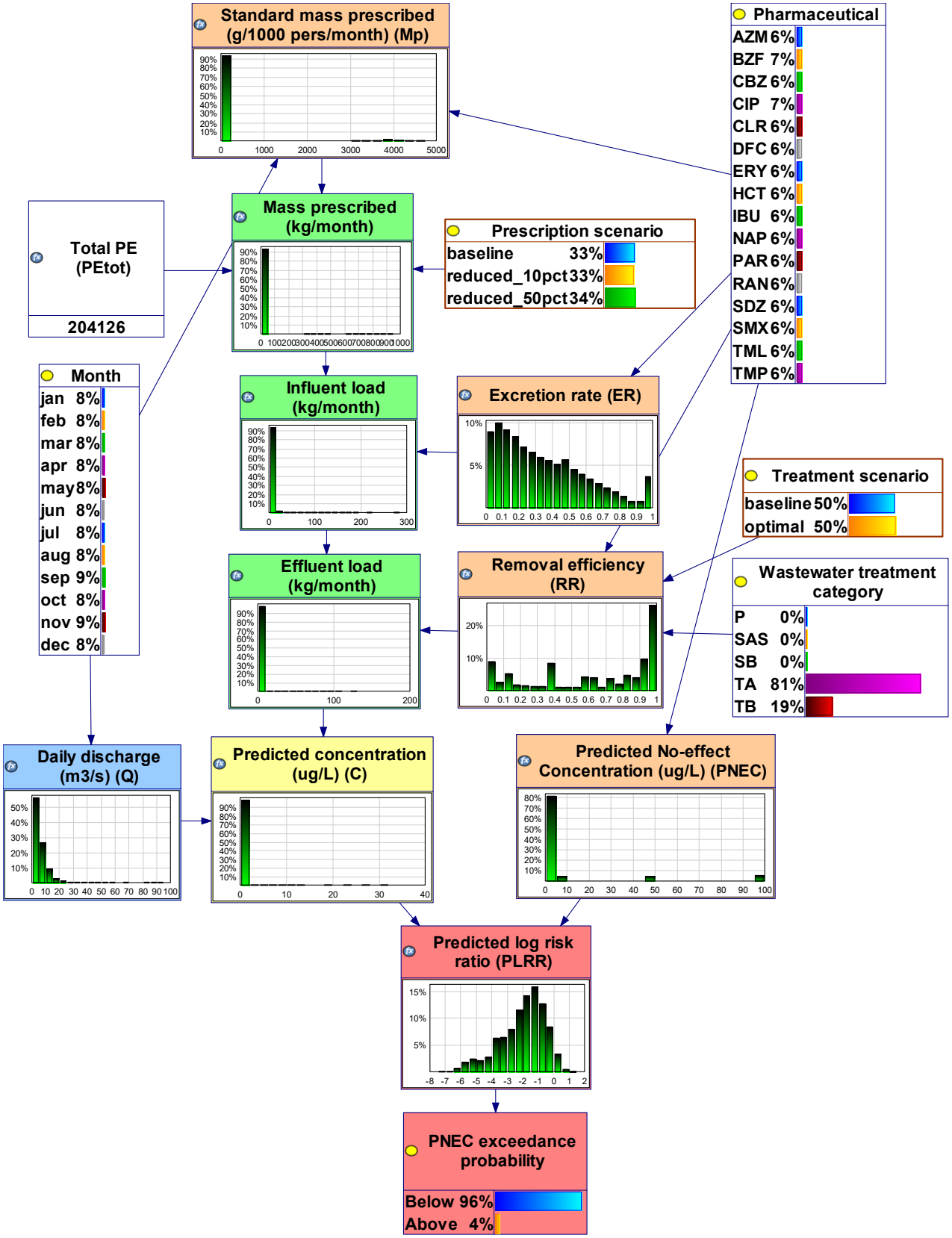

Figure 1. BN for simulating pharmaceutical concentration and risk of exceeding PNEC at a given monitoring point (here: MP1, see section 2.2) in a river catchment.

2.2 Study site

The model was applied to the River Almond catchment in West Lothian, Scotland (Figure 2). The main stem of the river is about 48 km long, with a catchment size of 375 km^2. The River Almond is typical of a UK system affected by significant shifts in economic development (from coal and oil shale mining to electronics and chemical industries, agricultural intensification, and urbanisation) since the mid-19th century, resulting in a gradient of pollution hotspots and impairments, a complex mixture of urban and fluvial flood risks, road runoff and challenges around CSO spills. These multiple pressures prevent the river from reaching good ecological status (SEPA, 2011). Sewage pollution has been identified as a significant problem, with the entire main stem of the Almond and several of its tributaries impacted by point source sewage pollution. There are 13 wastewater treatment facilities operated by Scottish Water within the catchment (Figure 2) ranging in size from <100 to ~120,000 population equivalents (PE) (Scottish Water, personal communication, January 30, 2024). The eight largest facilities (>4000 PE) are sewage treatment works (STWs) employing tertiary treatment, while the smallest are essentially large community septic tanks (see Table S2.1). Across the catchment, there are large rural areas where sewage treatment is served by private septic tanks systems.

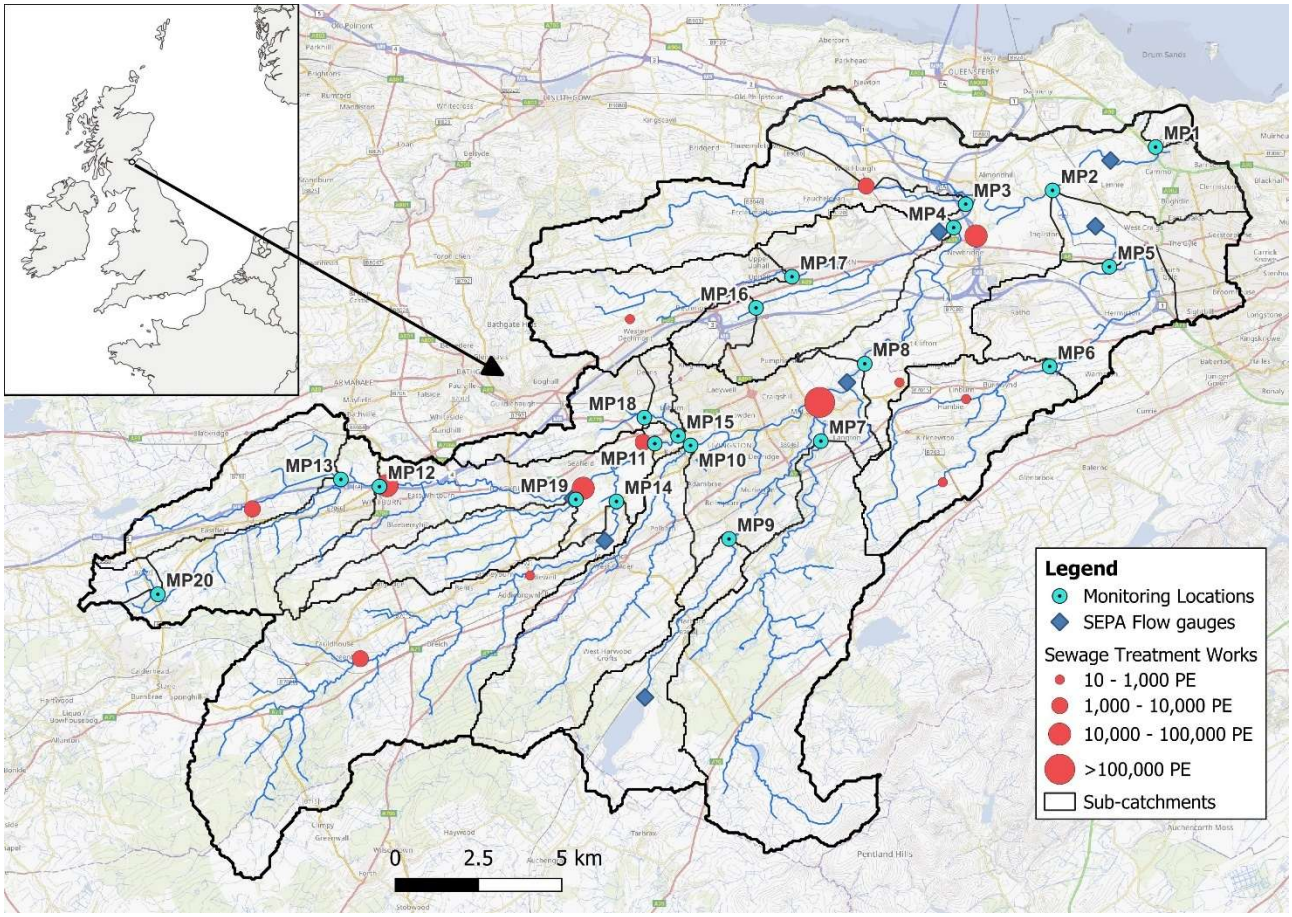

Figure 2: Catchment map showing the location of the 20 monitoring points in the Almond catchment (MPs), the 13 STWs, and the 5 flow gauging stations. © Crown copyright and database right (2025). All rights reserved. The James Hutton Institute, Ordnance Survey Licence Number AC0000812928

In total, 16 pharmaceuticals were considered for the modelling (Table 1). A 16-month sampling campaign (September 2023 – December 2024) was initiated in the catchment providing monthly pharmaceutical concentration data at 20 monitoring points (MPs) for 12 of these target compounds. Four antibiotics (azithromycin, ciprofloxacin, clarithromycin and erythromycin) were included in the

original list of target compounds, but these monitoring data were not available as part of this modelling study. The monitoring locations are shown in Figure 2. Table 2 summarises the number of STWs and total PE within the sub-catchments of each MP as well as the density of private septic tanks (SEPA, personal communication, November 6, 2025), the density of combined sewer overflow (CSO) outfalls (Scottish Water, personal communication, October 7, 2024), and land cover distribution (Rowland et al., 2025). Note that the information on private septic tanks, CSO outfalls and land cover is not included as input in the modelling but provided as an indication of where other sources of pharmaceutical pollution may be present in the catchment.

Table 1. Overview of the 16 target compounds included in the modelling, showing compound name and acronym, Chemical Abstracts Service (CAS) number, therapeutic class, usage type (H = human, V = veterinary, excluding non-livestock) and predicted no-effect concentration (PNEC) used for ecological risk assessment. Veterinary usage based on VMD (2025).

Compound	**CAS**	**Class**	**Usage**	**PNEC (µg/l)**
Azithromycin (AZM)	83905-01-5	Antibiotic	H	0.019
Bezafibrate (BZF)	41859-67-0	Lipd regulator	H	2.3
Carbamazepine (CBZ)	298-46-4	Antiepileptic	H	2
Ciprofloxacin (CIP)	85721-33-1	Antibiotic	H	0.064
Clarithromycin (CLR)	81103-11-9	Antibiotic	H	0.12
Diclofenac (DFC)	15307-86-5	Anti-inflammatory	H	0.04
Erythromycin (ERY)	114-07-8	Antibiotic	H + V	0.3
Hydrochlorothiazide (HCT)	58-93-5	Diuretic	H	100
Ibuprofen (IBU)	15687-27-1	Anti-inflammatory	H	0.011
Naproxen (NAP)	22204-53-1	Anti-inflammatory	H	1.7
Paracetamol (PAR)	103-90-2	Analgesic & antipyretic	H + V	46
Ranitidine (RAN)	66357-35-5	H2 blocker	H	3.1
Sulfadiazine (SDZ)	68-35-9	Antibiotic	H + V	1
Sulfamethoxazole (SMX)	723-46-6	Antibiotic	H + V	0.6
Tramadol (TML)	27203-92-5	Opioid analgesic	H	8.65
Trimethoprim (TMP)	738-70-5	Antibiotic	H + V	0.5

Note: Twelve compounds were selected because they were detected >10% occurrence during our monitoring campaign. Azithromycin, ciprofloxacin, clarithromycin and erythromycin were added as they are on the WHO AWaRe watch list for broad-spectrum antibiotics with higher resistance potential.

Table 2. Overview of number of STWs, total population equivalent (PE), density of private septic tanks (STs/km^2), density of combined sewer overflow outfalls (CSOs/km^2), and land cover distribution within the sub-catchment to each monitoring point (MP).

MP	No. of STWs	Total PE	ST density	CSO outfall density	Land cover (%)						
					Wood-land	Arable	Improved grassland	Semi-natural grassland	Mountain, heath & bog	Water	Built-up
1	13	204126	4.1	1.2	23.3	17	27.6	2.3	11.7	0.6	17.5
2	2	114	9.5	0.5	10.9	32.7	30	1.1	0.4	0.1	24.7
3	1	4578	5.4	1.0	13.2	39.3	40.5	0.8	1.2	0.1	5
4	1	9	5.5	2.4	16.2	23	29.4	1.2	2.2	0.2	27.9
5	2	114	11.8	0.7	13.4	39.9	33.8	1.3	0.5	0.1	11.2
6	2	114	12.7	0.7	14.5	28.5	47	2	0.7	0.1	7.1
7	0	0	1.4	0.0	30.6	0.9	17.7	6.1	43	1	0.8
8	7	168359	2.5	1.2	29.9	4.7	28.4	3.2	18.6	0.8	14.3
9	0	0	3.3	0.1	27.3	2.5	27.8	0.4	32	8.7	1.3
10	0	0	4.1	1.3	33.9	5.9	40.7	0.5	7.8	0.1	11
11	6	50837	3.0	0.9	31.3	4.7	34.5	4.2	15.4	0	9.9
12	1	3945	2.2	0.6	32.4	1.1	36.9	0.5	19.4	0	9.7
13	1	3945	3.9	1.1	33.7	0.2	37.7	0.2	18.7	0	9.6
14	2	5393	2.8	0.7	39.5	1.2	27.1	8.1	17.9	0	6.3
15	0	0	0.5	1.7	25.6	16.7	11.4	0	1.5	0.5	44.3
16	0	0	3.5	2.4	19.7	8.1	28.6	0.2	0	0	43.4
17	1	9	3.6	1.7	17.6	18.1	46.8	1.8	1.3	0.5	14
18	0	0	0.6	0.0	25.4	19.6	11.3	0	1.9	0.4	41.4
19	0	0	4.8	0.3	11.6	7.7	70.1	1.9	6.4	0	2.5
20	0	0	1.8	0.0	6.9	0	36.6	3.5	52.6	0	0.4

2.3. Data sources

The BN model was applied at each of the 20 monitoring points (MPs) to simulate the concentration and risks of the 16 pharmaceuticals. The sub-catchments at each MP were delineated to identify STWs located upstream of the MP. The location, amount of wastewater treated (in people equivalents), and the treatment type of each STW within the catchment was provided by Scottish Water (Scottish Water, personal communication, January 30, 2024). These parameters were considered as deterministic inputs in the model and are shown in Table S2.1.

In the following, we describe the remaining data sources used and the processing carried out to derive the parameter inputs for the BN model.

2.3.1. Prescribing rates

Monthly standardised masses prescribed (g/1000 people) between 2019–2024 were derived from the Public Health Scotland Prescribing Information System (PIS) database (PHS, 2025). PIS holds 100% of NHS Scotland prescriptions dispensed within the community and claimed for payment by a pharmacy contractor (i.e. general practices (GPs), community pharmacies, dental clinics and hospitals).

The monthly standardised prescription rates between 2019-2024 were summarised by NHS health board area. This allowed us to include the prescribing contribution from hospitals and dental clinics, which is only available aggregated at health board level.

Mean and standard deviation of the standardised prescription rates were calculated by month and health board and used as input for the BN model, assuming the monthly prescription rates to follow a normal distribution. The study catchment is located in NHS Lothian, hence the summarised prescribing data for this health board was used as input for the final BN model.

Further details about the derivation of the prescribing rates can be found in S2.2.

2.3.2. Excretion rates

Excretion rates were required to estimate the proportion of each prescribed pharmaceutical entering the wastewater system. For the purposes of this study, we sought to represent the total excretion of unchanged compound, i.e. the sum of excretion via both urinary and faecal routes. As noted in Jagadeesan et al. (2025), many studies only account for urinary excretion rates when estimating the pharmaceutical loads via sewage and hence may exclude significant contributions from faecal excretion. This was also the case in the study by Niemi et al. (2024) who applied Bayesian Belief Network modelling for Scotland-wide prediction and mapping of the environmental impact of selected pharmaceuticals in freshwater catchments. Including the faecal contribution is conceptually straightforward but practically challenging, since most published pharmacokinetic data report only urinary excretion, and not all clearly distinguish between unchanged, conjugated, and metabolised fractions.

A literature review was undertaken to compile excretion data for the 16 target pharmaceuticals. Information was extracted from pharmacokinetic studies, drug monographs (e.g. Martindale: The Complete Drug Reference), and online resources such as DrugBank (Knox et al., 2024; https://go.drugbank.com/) and RxList (https://www.rxlist.com/). For several compounds, the recent reviews of excretion rate data by Holton et al. (2022), Kannan et al. (2023) and Ceolotto et al. (2024) could be utilised. When multiple sources were available, all reported values were collated to characterise the observed range and variability. Particular attention was paid to whether reported data referred explicitly to excretion of the unchanged parent compound, to both unconjugated and conjugated fractions, or to total recovery in excreta. In some studies, this distinction was unclear, which likely contributes to the substantial spread of reported values in the literature. The collated removal rates are summarised in Figure S2.3.

For compounds where faecal excretion was poorly quantified but known to be significant, total excretion was approximated as the sum of the urinary excretion of unchanged compound and the fraction of the administered dose not absorbed during ingestion, the latter being assumed to represent biliary elimination. Conversely, where urinary recovery accounted for nearly all of the administered dose, urinary data were taken as a proxy for total excretion. This approach ensures that both the renal and faecal/biliary pathways are represented consistently across compounds.

The collated excretion data reveal wide variability among studies and among compounds, reflecting differences in study design, analytical methods, and inter-individual pharmacokinetic variability (e.g. age, renal or hepatic function). To propagate this uncertainty within the BN, probability distributions were derived for each pharmaceutical based on the collated excretion data. Beta distributions were selected, because they are flexible and constrain values between 0 and 1. The parameters of each distribution were estimated using the method of moments based on the mean and variance of the collated data (Soch, 2020), and using the number of subjects involved for each study as weights (as also done in Ceolotto et al., 2024; Holton et al., 2022; Kannan et al., 2023). These distributions

therefore represent the plausible range of total unchanged excretion fractions, capturing both measurement uncertainty and true biological variability.

The compiled dataset is provided in the accompanying code repository (see Data and code availability).

2.3.3. STW removal efficiencies

Removal efficiencies were required to estimate the fraction of each pharmaceutical load that remains in treated effluent and ultimately enters the receiving water. The removal of pharmaceuticals during wastewater treatment is complex and highly compound- and process-specific, influenced by factors such as sewage composition, plant design and operation, hydraulic and solid retention times, environmental conditions, and the physicochemical properties of the compound (Clara et al., 2005; Petrie et al., 2015; Zorita et al., 2009). To characterise these processes probabilistically, removal efficiencies were collated from both the scientific literature and from large-scale monitoring data obtained under the UK Chemical Investigations Programme (CIP) for Scotland (OHBP, 2025) and for England & Wales (UKWIR, 2025).

From the literature, studies reporting paired influent and effluent concentrations of pharmaceuticals from full-scale STWs were extracted. For each pharmaceutical, the reported removal efficiency was recorded as the percentage change in concentration (or load, if available) between influent and effluent. In parallel, paired influent and effluent concentration data for the 16 target pharmaceuticals were extracted from the CIP datasets, covering a total of 30 wastewater treatment works in Scotland and 56 in England and Wales. Information on treatment configuration was derived from Scottish Water's annual return data (Scottish Water, personal communication, January 30, 2024), and, for England and Wales, from public registers from the Water Services Regulation Authority (Ofwat) and the Urban Wastewater Treatment Directive (UWWTD) (Environmental Agency, 2016).

To enable the parameterisation of the BN model, all treatment works were classified into five treatment categories consistent with those used by Scottish Water and in the UWWTD: Primary (P), Secondary Activated Sludge (SAS), Secondary Biological (SB), Tertiary Activated Sludge (TA), and Tertiary Biological (TB). This classification facilitated grouping of heterogeneous datasets into a manageable number of categories while retaining the key process differences between activated sludge and biological filtration systems, and between secondary and tertiary levels of treatment. The final classification is summarised in Table S2.4.

For each pharmaceutical–treatment category combination, the collected removal efficiencies were summarised and fitted using beta probability distributions bounded between 0 and 1, as for excretion rates in 2.3.2 above. The parameters of each distribution were again estimated using the method of moments from the mean and variance of the collated data as described above. These distributions were then used as prior inputs to the BN model.

For combinations of pharmaceuticals and treatments with very limited or no empirical data, removal rates were inferred from other treatment categories or assumed from structurally and behaviourally similar compounds. In particular, data for primary treatment were sparse and inconsistent - sometimes even indicating higher removal than secondary or tertiary systems, which is unlikely - so removal during primary-only treatment was conservatively assumed to be negligible.

The resulting dataset is shown in Figure S2.4 and revealed a wide range of behaviours: some pharmaceuticals (e.g. ibuprofen, paracetamol, naproxen, sulfadiazine) were consistently well removed (>80%) in secondary and tertiary treatment, whereas others (e.g. carbamazepine,

tramadol) were persistent with negligible removal (<5%). For many compounds the degree of removal increased with higher treatment level (secondary to tertiary). Removal efficiencies also appear to depend on treatment type, with some compounds more effectively removed with activated sludge (e.g. clarithromycin, erythromycin), while biological (filtration) treatment was more effective for others (e.g. diclofenac, trimethoprim). Other compounds (e.g. bezafibrate, carbamazepine) showed little dependence on treatment level and type.

The compiled dataset on removal efficiencies is provided in the accompanying code repository (see Data and code availability).

2.3.4. River flow

River discharge in the study catchment is monitored at five gauging stations by the Scottish Environmental Protection Agency (SEPA) (Figure 2). A hydrological model of the catchment was set up using SWAT (Soil & Water Assessment Tool) and calibrated against the observed daily river discharge data from the flow gauges. Calibration was performed for the period January 2021 to December 2022, while validation covered January 2023 through May 2024. The model achieved a Kling-Gupta efficiency (KGE) of 0.756 Nash –Sutcliffe Efficiency (NSE) of 0.635, and a PBIAS of −10.0 %, indicating good agreement with observations and a slight underestimation of flow. During validation, the model maintained reasonable performance (KGE = 0.703, NSE = 0.654) with a PBIAS of −15.2 %, suggesting a continued tendency to underestimate flows (Corrochano-Fraile et al., in review).

The calibrated model was used to simulate current, baseline and future flows at the 20 ungauged monitoring points. This study utilises high-resolution precipitation and temperature projections from UK Climate Projections 18 (UKCP18) to assess future climate impacts, using Representative Concentration Scenario (RCP) 8.5, an emissions-intensive scenario. Timeseries precipitation and temperature data were used to drive the models from 1980 through to 2080. The UKCP18 projections are available at 2.2 km grid resolution, simulating climate dynamics at a local scale. The 12 climate projection ensembles were bias corrected using quantile mapping to observed data in the catchment. This gave 12 possible future timeseries realisations of flow for each of the 20 monitoring points.

The modelled daily flow timeseries for each monitoring point from January 2021 – May 2024 were summarised as log-normal distributions by month and inputted to represent the current climate situation in the BN model. Similarly, the 12 possible realisations of the daily flow timeseries were summarised as monthly log-normal distributions for, respectively, a baseline period (1990-2020) and a future reference period (2050-2080) and used as input for the BN model to examine the possible effects of future climate change.

2.3.5. Ecotoxicity thresholds

Lowest available PNEC values in freshwater for each target pharmaceutical (Table 1) were taken from the Norman Ecotoxicological database (https://www.norman-network.com/nds/ecotox/) (Norman, 2025). The PNEC values were assumed constant/fixed in the modelling.

2.3.6. Field sampling and pharmaceutical analysis

The 20 monitoring locations (Figure 2) included five sites on the River Almond main stem and the remainder on its major tributaries, spanning the catchment from near the source of the Almond to its confluence to the Firth of Forth. Water samples were collected monthly between September 2023 and December 2024. The samples for pharmaceutical measurement were collected in 1 litre glass Duran bottles. These samples were preserved with 3 ml of 1.5M sodium azide upon return to

the laboratory and kept refrigerated prior to analysis. Analysis for pharmaceuticals was conducted by ultra-Performance Liquid Chromatography coupled by tandem mass spectrometry (UPLC-MS/MS).

2.4 Model evaluation and handling of censored concentration data

Simulated concentration distributions were compared to the observed data for each pharmaceutical and sampling location combination to evaluate model performance. To quantify the correspondence between observed and simulated concentration distributions, two complementary distance metrics were calculated. The Jensen-Shannon divergence (JSD) distance was calculated to evaluate differences in distribution shape (Menéndez et al., 1997; Acker et al., 2025), while first Wasserstein (W1) distances (Vilani, 2009; Huyn et al., 2022) were computed on log10-transformed concentrations to quantify the average multiplicative deviation (bias) between observed and simulated distributions. The JSD and log-W1 distances were calculated by R functions distance() and wasserstein1d() from the R packages *philentropy* and *transport*, respectively. Table S2.5 summarises typical interpretation thresholds for the two metrics. For log-W1, values <0.3 indicate close agreement corresponding to less than a two-fold difference in concentration, while values around 1 denote differences of approximately one order of magnitude.

For some pharmaceuticals and locations, a substantial proportion of the observed concentrations were reported below the analytical limit of detection (LOD) (section 3.1). To ensure consistent treatment of censored observations, measured concentrations below LOD were treated as left-censored and replaced at LOD/2, which provides an unbiased mid-point estimate under uniform censoring. Note that as JSD become less sensitive when a large proportion of observations are censored, model–data comparison emphasised log-W1, which is more robust to censoring.

2.5 Risk characterisation and scenarios

For each compound, monitoring point, and month, the BN simulates a posterior probability distribution of concentrations. Based on this, the risk is then quantified as the probability of exceeding the PNEC. Results were mapped for the 20 MPs and for an additional 18 points along the river system to facilitate interpretation of risk levels for refined river reaches.

To explore the impact of management and climate change, the following scenarios were explored:

(i) Reducing prescribing rates by 10% and 50%, respectively. This was done by introducing a ‘Prescription scenario’ node in the network, which multiplies the prescription rates by 0.9 and 0.5 depending on the chosen scenario.

(ii) Increasing STW removal efficiencies to ‘optimal’. This was implemented by introducing a ‘Treatment scenario’ node that fixes the removal efficiency for each compound–treatment category at its respective 90th percentile value, based on the compiled literature-derived removal distributions. This effectively represents performance comparable to the best-performing STWs reported in the literature. In the results, this is referred to as the ‘optimal’ treatment scenario.

(iii) A 'maximum' scenario combining 50% reduction in prescribing rates and 'optimal' STW removal efficiency.

(iv) Using the future river flow projections, based on UKCP18 RCP 8.5 to represent a reasonable worst-case climate scenario (see section 2.3.4).

3. Results and Discussion

3.1 Observed pharmaceutical concentrations

Figure S3.1 shows the observed concentrations of the twelve pharmaceuticals included in the sampling campaign at each of the 20 monitoring points (MPs) across the catchment between September 2023 and December 2024. Table S3.1 summarises the observed detection frequencies by sampling location. Across the catchment, the twelve monitored compounds have been observed above the Limit of Detection (LOD) in at least 10% of the samples taken, except hydrochlorothiazide (HCT) (7%). While all the pharmaceuticals are detected in the catchment, only ibuprofen (IBU) (61% of all samples), diclofenac (DFC) (19% of all samples), and sulfamethoxazole (SMX) (0.3% of samples) have been observed above their respective no-effect concentration values (Figure S3.1).

The most frequently detected pharmaceuticals across the catchment were IBU, carbamazepine (CBZ), naproxen (NAP), paracetamol (PAR), and tramadol (TML), all of which have been detected in over 60% of the samples. This aligns with the prescribing data, which show that these five compounds are also the ones prescribed at the highest rates (Figure S2.1 and S2.2). Spatially, pharmaceutical pollution (above LOD) has been detected at all MPs, with at least three pharmaceuticals detected in over 10% of the samples at every MP in the catchment, and with the majority of the MPs detecting at least 8 pharmaceuticals. MP1, MP8 and MP11 along the main stem of the river are the locations most impacted by pharmaceuticals, with all 12 pharmaceuticals being detected in over 10% of the samples. This agrees with the wastewater treatment work information (Table 2), which shows that these three MPs are the locations receiving the highest volumes of treated wastewater (in PE). However, elevated pharmaceutical concentrations have also been observed in sub-catchments without known STWs. For example, MP19 showed some of the highest NAP concentrations recorded in the catchment and concentrations of both IBU and DFC occasionally exceeding their respective PNEC values, despite no identified STW inputs. Given the catchment for MP19 is heavily agricultural (Table 2) and that none of these three compounds are for veterinary use (Table 1), this likely points to inputs from poorly maintained private septic tanks. Conversely, several headwater MPs (7, 9, 10, 15, 16, 18, 20) with no known STW inputs showed consistently low concentrations, often below detection limits, supporting the dominant role of STWs where they are present.

3.2 Model performance and comparison with monitoring data

The Bayesian Network was applied to simulate the pharmaceutical concentrations at the 20 monitoring points in the catchment. However, only twelve of the MPs are impacted by STWs discharges (Table 2), hence the simulated results are only shown for these twelve MPs here. For all other MPs, the simulated concentration values are zero.

Figure 3 shows the simulated concentration distributions compared against the observed data for each pharmaceutical and sampling location combination. Figure S3.2-S3.3 shows heatmaps of the distance metrics by pharmaceutical and sampling location.

Simulated concentration distributions generally compared well with observed data across most pharmaceuticals and locations (Figure 3). The log-scaled Wasserstein distances typically ranged between 0.3 and 1, corresponding to median absolute deviations of less than one order of magnitude between observed and simulated values, indicating that the model reproduced the concentration distributions satisfactorily. The agreement is particularly evident for tramadol (TML), trimethoprim (TMP) and sulfamethoxazole (SMX), where log-scaled W1 values were below 0.5 across most locations; the model also generally performed well for carbamazepine (CBZ), diclofenac

(DFC) and paracetamol (PAR). JSD values were typically < 0.1, both indicating moderate to strong similarity between observed and simulated probability distributions (Figure S3.3).

However, some of the pharmaceuticals deviate from the above pattern. Sulfadiazine (SDZ), ibuprofen (IBU) and, to a lesser extent, hydrochlorothiazide (HCT) appear to be consistently underestimated by the model, suggesting that the STW loadings were underestimated, likely due to underestimation of the amount prescribed, underestimation of the excretion rate, and/or overestimation of the removal efficiency. However, the detection rate of HCT in the river samples is low (7%), which makes the comparison to the simulated values more difficult. In fact, most of the simulated HCT values are below the LOD, in agreement with the low observed detection rate of HCT. SDZ is a widely used veterinary medicine, which could explain the underestimation, especially in catchments dominated by agriculture. For IBU, the underestimation is likely due to the omission of over the counter (OTC) consumption, which is expected to be substantial. For example, Austin et al. (2021) estimated OTC sales of ibuprofen to make up 76% of the total mass of ibuprofen sold or prescribed in the UK. In contrast, for paracetamol (PAR), another non-prescription drug, the simulated concentrations are more in line with the observed ones. The simulated ranitidine (RAN) concentrations appear to be overestimated and display a much larger spread compared to the observed concentrations. RAN was previously available over the counter in the UK but was banned from use in 2020 and has seen a dramatic decrease in prescription rates since (Figure S2.2). It is therefore likely that the prescription rate distribution for RAN (Figure S2.1), derived based on prescription data from 2019-2024, has been overestimated.

Spatially, the model performed best at MPs located along the main river stem, which receive the largest contributions from STWs (i.e., MP1, MP8, and MP11). Here, simulated and observed concentrations aligned closely across most pharmaceuticals. Conversely, locations MP2, MP4, and MP17 in the tributaries consistently exhibited the largest log-scaled W1 values, suggesting systematic bias between observed and simulated concentrations. The concentrations at MP4 and MP17, both of which are only impacted by a small STW (Table 2), were consistently underestimated for all pharmaceuticals, indicating that additional, unaccounted sources such as private septic tanks and CSOs (Table 2) may be contributing. Despite clear visual differences between observed and simulated distributions at MP17 (Figure 3), the JSD metric suggested high correspondence (JSD < 0.001). This apparent discrepancy reflects the dominance of censored (<LOD) data at MP17, resulting in small distributional variance of observations and causing an entropy-based measure like JSD to underestimate discrepancies in shape or central tendency (Ren et al., 2025). MP2, located on the same tributary as MP5 and MP6, was also consistently underestimated despite the latter two being better reproduced. This points to possible unaccounted sources along the stretch between MP5 and MP2.

In summary, the model is deemed to perform well, with the distance metrics collectively suggesting that it satisfactorily reproduces the observed variability and distributional shape of pharmaceutical concentrations across most locations, with exceptions at a few sites (notably MP2, MP4 and MP17) and for certain compounds (notably SDZ and IBU). Overall, this indicates that the STWs in the catchment represent the dominant source of the observed pharmaceutical pollution in the river and that detailed prescribing data combined with STW information provide reliable estimates of the pharmaceutical loading to the river system. This aligns with previous modelling studies identifying STW effluents as the principal contributor to pharmaceutical loads in rivers (Jagadeesan et al., 2025; Oldenkamp et al., 2018; Wu et al., 2025).

However, as discussed in section 3.1, several monitoring points without any upstream STWs nevertheless exhibited detectable pharmaceutical concentrations (Table S3.1), and at these

locations the BN model predicts zero concentrations by design. Ibuprofen (IBU) and paracetamol (PAR) were detected above LOD in over 10% of the samples at all non-STW sites, while naproxen (NAP), sulfadiazine (SDZ), carbamazepine (CBZ) and tramadol (TML) were also frequently observed. These observations clearly indicate the presence of additional, unmodelled sources of pharmaceuticals within the catchment. One explanation could be episodic discharges from CSOs during high-flow or storm events. Such overflows can occur at several points within the drainage operating areas (DOAs) of the STWs, also upstream of monitoring points that have no STWs within their sub-catchment area (Table 2). Several of the frequently detected compounds (IBU, PAR, NAP and SDZ), present at non-STW sites, exhibit some of the highest removal efficiencies in wastewater treatment (Fig. 2.4). Their detection could therefore indicate that untreated or partially treated wastewater inputs, such as CSOs, emergency bypasses or sewer cross-connections may contribute to localised contamination during rainfall events.

Another important pollution pathway is likely to be private septic tank systems that are widespread in the catchment (Table 2) and currently not represented in the model. Septic tanks can discharge pharmaceuticals continuously at low levels, particularly where systems are poorly maintained or hydrologically connected to surface waters (Ramage et al., 2019). This mechanism provides a plausible explanation for the broad suite of compounds detected at some non-STW sites, particularly at MP19, where elevated concentrations of a range of pharmaceutical are detected, despite no STWs or CSOs located upstream. In addition, diffuse rural sources are also likely to play a role. Agriculture is a dominant land use within the catchment (Table 2), and some of the compounds detected at MPs with no STWs upstream are used in veterinary medicine (e.g., SDZ and PAR; Table 1). Inputs from land application of manure, slurry and/or sewage sludge could therefore contribute to pharmaceutical presence.

Overall, the presence of pharmaceuticals at non-STW monitoring points highlights the importance of sources that are not captured by STW-based modelling alone and underline the need for future model development to include septic systems, sewer overflows and agricultural pathways to fully represent pharmaceutical inputs at catchment scale.

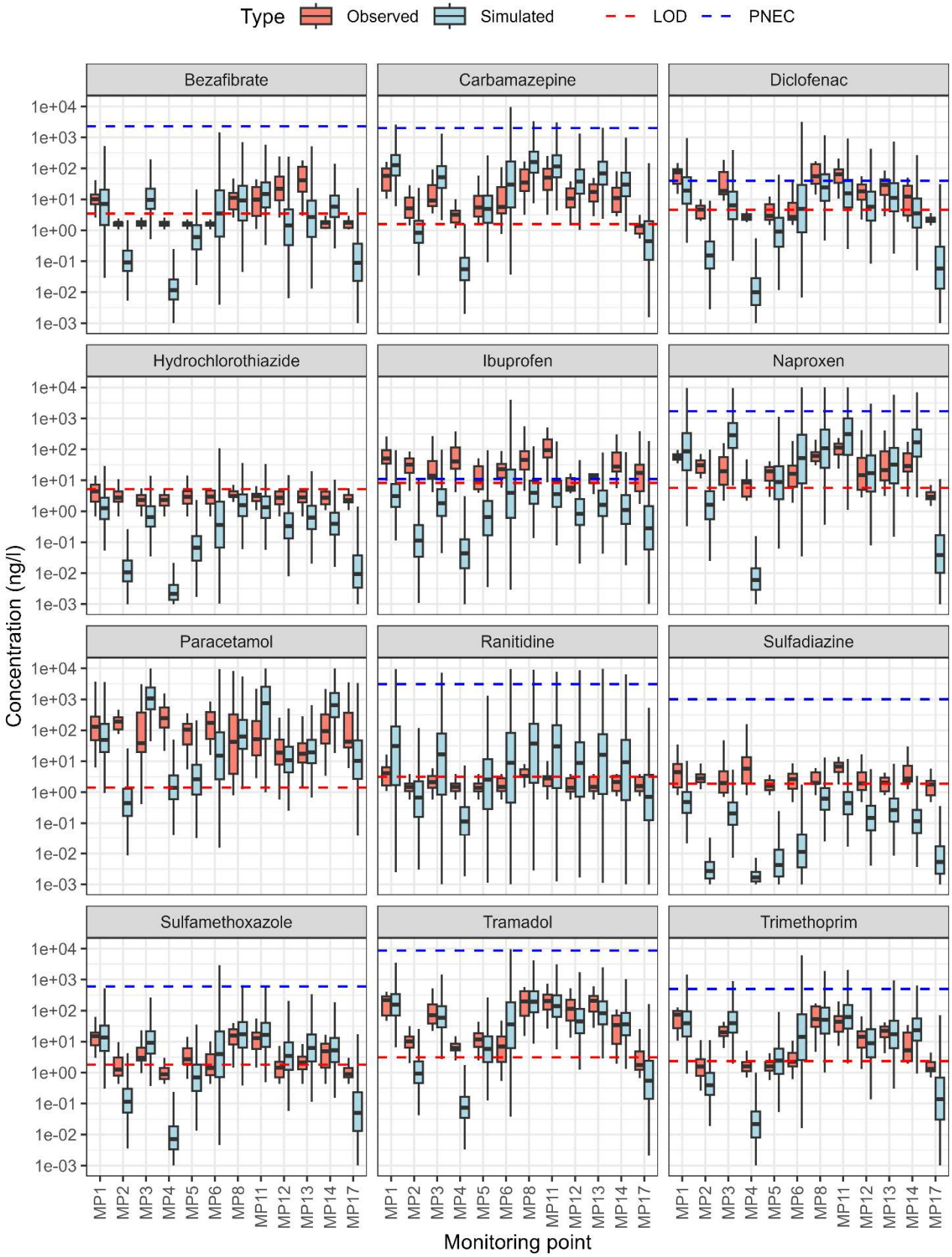

Figure 3: Observed vs simulated concentrations of 12 target compounds at 12 locations in the catchment. Note, PNEC for hydrochlorothiazide (HCT) and paracetamol (PAR) are outside the scale of the plot and not shown (See Table 1).

3.3 Risk assessment

Pharmaceutical risks were quantified as the probability of concentrations exceeding predicted no-effect concentrations (PNECs). Figures 4 and 5 show the simulated risk of diclofenac (DFC) spatially by month. The simulated risks for a selection of other compounds are shown in Supporting Information S3.3.

Simulated concentrations and risks displayed clear seasonal patterns linked to hydrology (Figures 4 and 5). Concentrations and exceedance risk were generally lower in late autumn and winter when river flows were high, and higher in summer during low-flow conditions. This pattern highlighted the role of dilution in controlling pollution risk and shows that most of the pharmaceuticals display point source behaviour.

The highest risks were associated with AZM, DFC, IBU, and CLR (Figure 4, Figures S3.4-S3.7). For these compounds, the probability of exceeding PNECs at heavily STW-impacted sites (e.g. MP1, MP8, MP11) exceeded 50% during the summer months. In contrast, compounds such as bezafibrate (BZF), hydrochlorothiazide (HCT), sulfadiazine (SDZ), tramadol (TML), and sulfamethoxazole (SMX) exhibited little or no risk throughout the year. In general, seasonal dilution effects were clear, with the predicted risks markedly reduced during the wetter winter months.

While the highest risks were generally predicted in the lower parts of the catchment where treated wastewater volumes are greatest, some smaller headwater catchments also exhibited elevated risks during the summer months, despite receiving much smaller volumes of wastewater (Figure 4). However, the dilution capacity in these tributaries is very low and particularly evident at MP6. This finding highlights that risk is not simply a function of pollutant loads, but of the interplay between loads and river flow (Corrochano-Fraile et al, in review).

It is worth noting that while the modelling work here finds that risks are reduced during high flows due to the increase in dilution capacity, it is well known that high rainfall events can also lead to increases in pollution loads due to e.g. sewer overflows, runoff and reduced residence times in STWs. These sources and effects are not currently included in the model and hence, the risks during episodic high rainfall events are not represented. The increase in risk during high rainfall will be pharmaceutical dependent, increasing more significantly for pharmaceuticals that are most effectively removed in wastewater treatment under normal flow conditions.

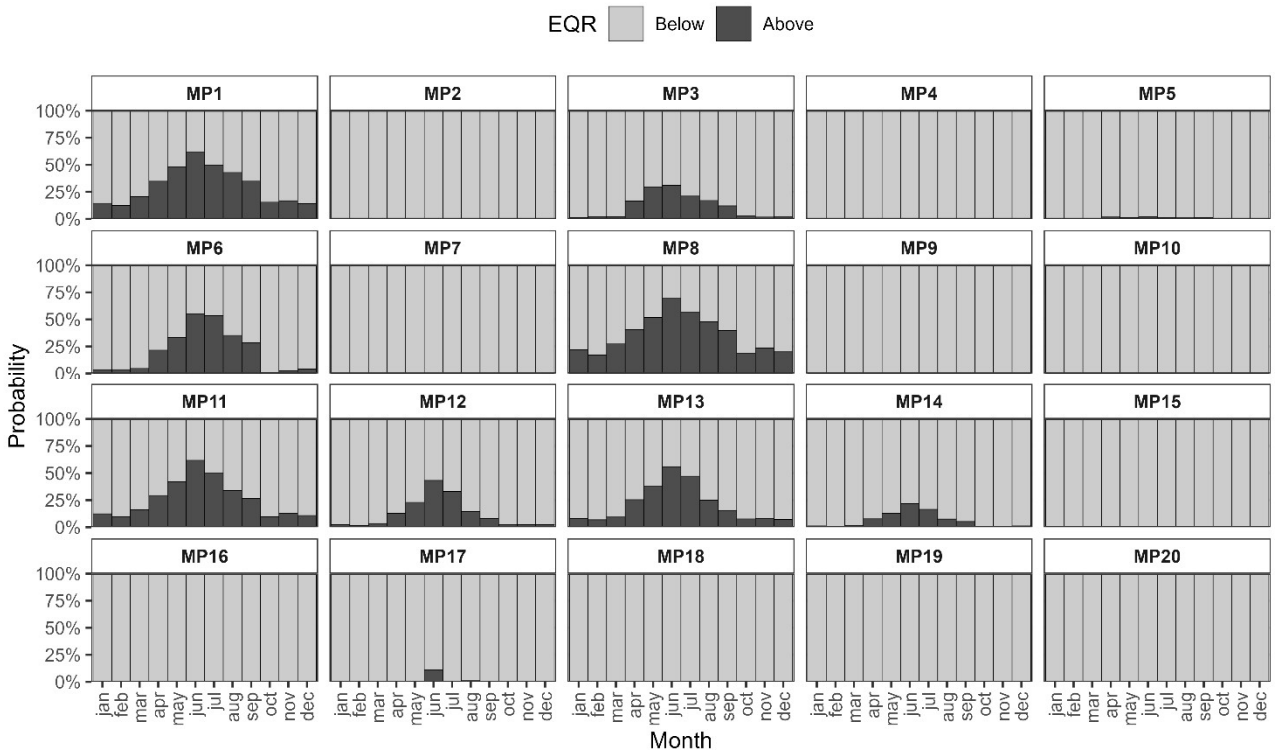

Figure 4: Example of simulated probability of exceeding the PNEC for diclofenac (DFC) as monthly bar plots.

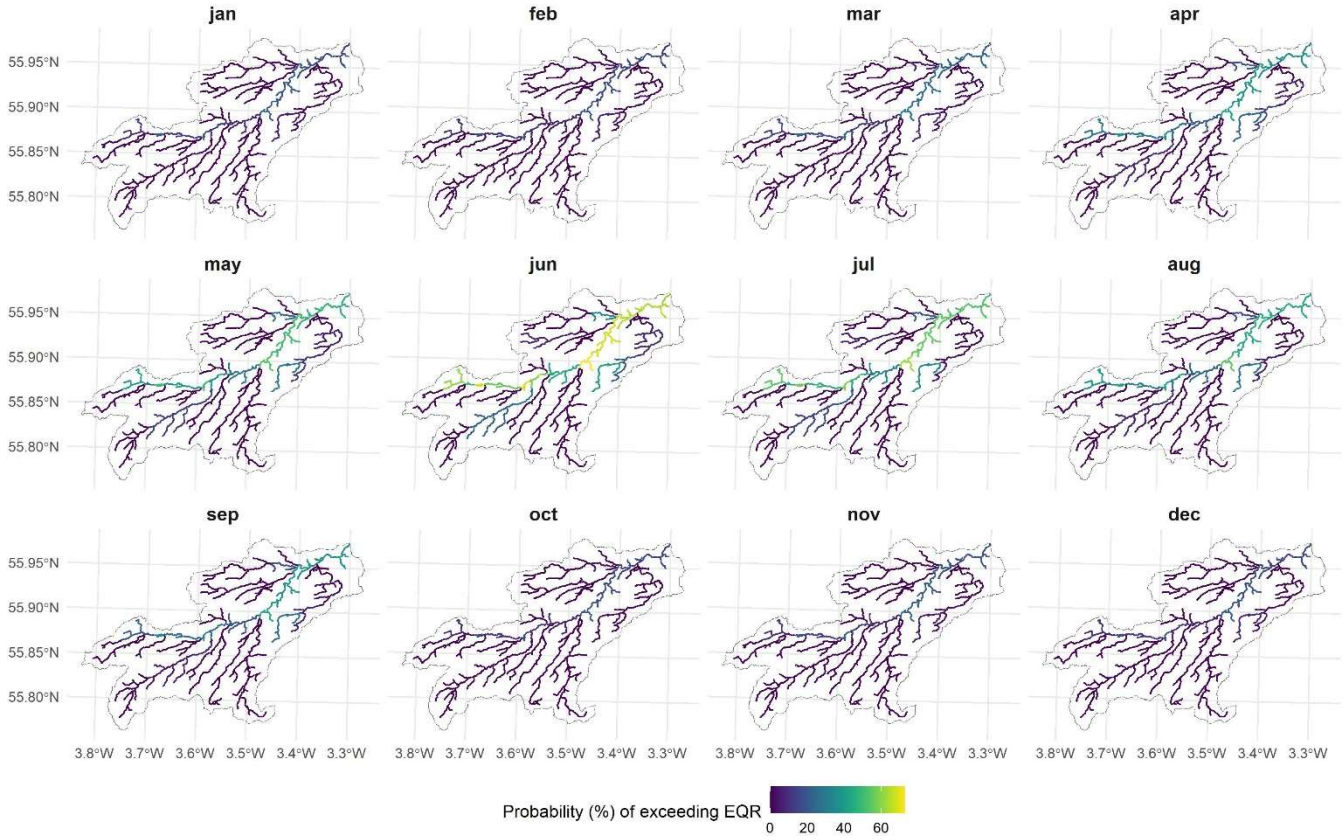

Figure 5: Example maps showing the simulated probability of diclofenac (DFC) exceeding the PNEC by month.

3.4 Scenario analysis

3.4.1 Impact of future climate change

The BN model was used to explore how future climate (UKCP18 RCP8.5) might affect the pharmaceutical pollution risks. To do this, the risk was evaluated and compared for a 30-year baseline climate period (1990-2020) and a 30-year future climate period (2050-2080) (see section 2.3.4). Figure 6 shows the predicted exceedance probabilities for carbamazepine (CBZ), clarithromycin (CLR), diclofenac (DFC) and ibuprofen (IBU) at sampling locations MP1 and MP6 for the current situation, using observed flow for period 2020-2024, and for the baseline and future climate scenarios, using simulated hydrological flow projections, as described in section 2.3.4 above. The results for all 16 compounds are shown in Figures S3.8 and S3.9.

Comparison of these hydrological climate change scenarios indicates contrasting behaviour between main-stem and headwater locations. Exceedance probabilities under the baseline scenario were somewhat higher than those derived using the current observed flow period during autumn months (Figure 6, Figure S3.8), possibly a reflection of the observation period, which recorded higher flows than the average baseline hydrological period (1990-2020). This was particularly evident in smaller headwater catchments, especially at downstream tributary sites such as MP6 (Figure 6, Figure S3.9) that exhibited substantially higher exceedance probabilities under the ensemble-based baseline scenario compared to current conditions. While this indicates strong sensitivity of risk to the representation of low-flow conditions, it also suggests that the current (2020–2024) observed period may have been relatively wet when comparing to the long-term average.

Compared to the baseline scenario, reduced summer and autumn flows under future scenarios (Corrochano-Fraile et al., in review) resulted in further increase in the predicted risks, with exceedances becoming more frequent and widespread. For example, the probability of CLR, DFC, and IBU exceeding the PNEC at MP1 in August increased from 31%, 55% and 36% in the baseline scenario to 46%, 68%, and 56% in the future scenario. The increase is generally most pronounced at monitoring points already characterised by elevated risk under current conditions, reflecting reduced dilution under projected lower summer and autumn flows. Winter exceedance probabilities show comparatively minor changes.

Overall, these findings suggest that pharmaceutical pollution risk is strongly linked to hydrological variability and will therefore be sensitive to projected climate changes that alter flow regimes. The predicted amplification of risk under future drier summers reinforces this conclusion.

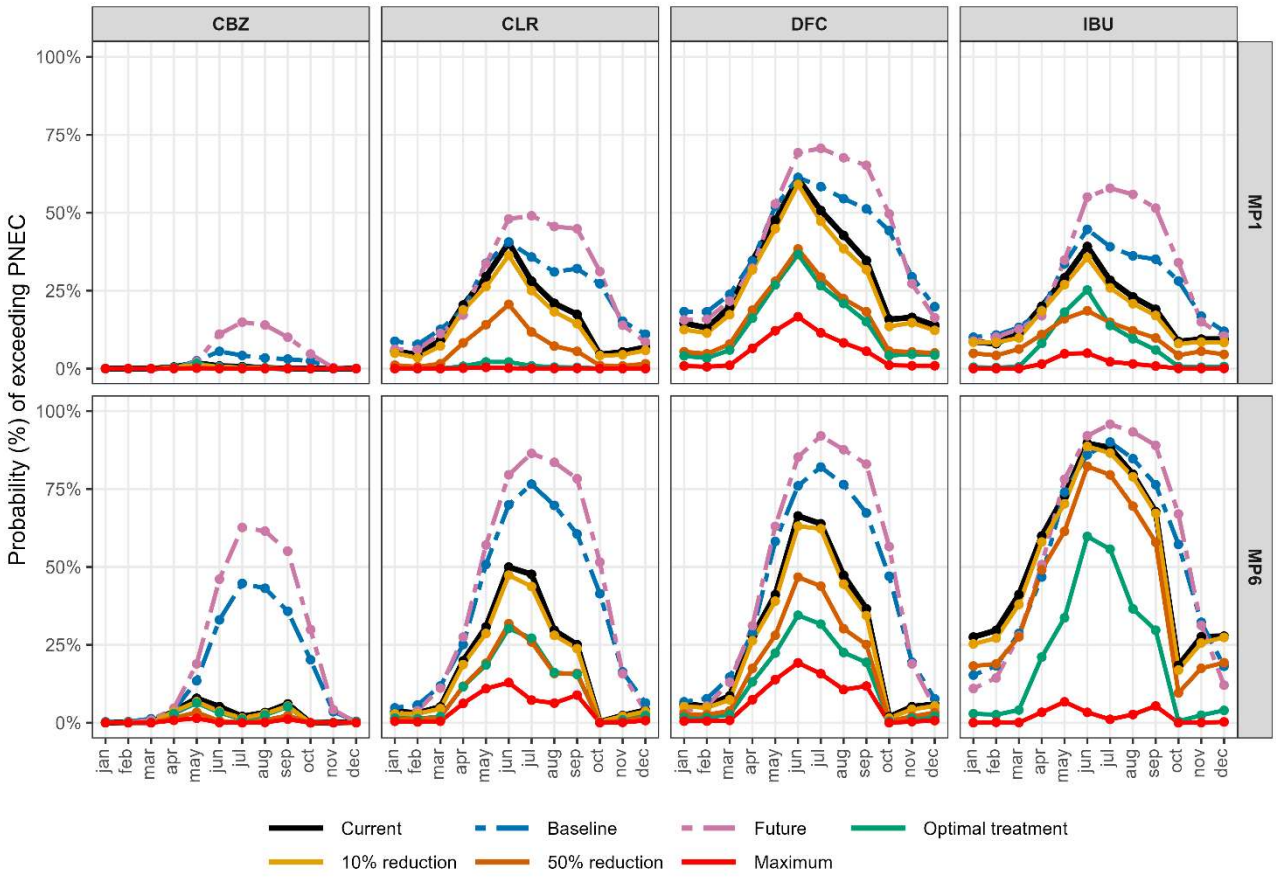

Figure 6: Simulated probability of exceeding the PNEC for four selected pharmaceuticals at sampling location MP1 (top panel) and MP6 (bottom panel) for the current (2020-2024), baseline (1990-2020) and future (2050-2080) climate periods, and for the four different management scenarios (optimal treatment, reduction in prescription rates by 10% and 50%, and a combined 'maximum' scenario; see section 2.5).

3.4.2 Impact of management

The management scenarios demonstrated the capacity of the model to quantify effectiveness of interventions. Figure 6 also shows the results of the management scenarios at location MP1 for the four selected compounds (Figure S3.10 shows the results for all 16 compounds). As clear from Equation 3, any reduction in the prescribed mass of pharmaceutical will lead to a proportionate reduction in the resulting concentrations and hence also to a reduction in the risk. For DFC, the peak risk was reduced from about 65% in the current case to 59% and 38% when the prescribing rates were reduced by 10% and 50%, respectively. Similarly, the peak risks of CLR and IBU were both reduced from about 43% in the baseline case to 36% and 20% following a 10% and 50% reduction in prescribing, respectively.

Figure 6 also shows the effect of all STWs in the catchment performing close to optimal (based on reported removal rates in literature) by fixing the wastewater treatment removal rates at the upper 90th percentile. The effect of this was found to be more compound specific. For example, the reduction in the risks of DFC at MP1 by using "optimal"' removal rates were similar to the reduction achieved by reducing prescribing rates by 50%. For CLR the risk reduction at MP1 was much more pronounced when using optimal treatment levels, with the peak risks of CLR being reduced from about 43% to 2%. However, the effect of using optimal treatment is also dependent on the monitoring location and the types of treatment works located upstream. The two STWs upstream

MP6 are both categorised as secondary biological (SB). The removal of CLR during SB treatment was found to be markedly lower (and with narrower range) compared to other treatment types (Figure S2.4), and hence the effect of using optimal treatment was more modest at MP6 compared to MP1 (and other monitoring locations where upstream sewage inputs were predominantly from STWs with tertiary treatment). Conversely, the effect of using "optimal" treatment was more modest for IBU at MP1 compared to MP6, because the reported removal values for IBU during tertiary treatment have a narrower range (Figure S2.4).

Note, that because the predicted concentrations are directly proportional to both the prescribing rates and the wastewater removal rates, it is straightforward to calculate the reduction in prescribing rates or increase in treatment removal rates required to ensure that PNEC values are not exceeded. For example, reducing AZM exceedance probability from ~80% to 10% in summer would require either a ten-fold reduction in prescribing rates or increasing STW removal to about 90% (from the current median removal values of ~10%). This required removal rate for AZM is significantly higher than has been reported in the literature. While such proportional scaling relationships can be derived analytically for prescribing or removal efficiencies separately, the BN provides a coherent approach for estimating the joint probability of PNEC exceedance under simultaneous uncertainty and variability in prescribing rates, removal efficiencies and hydrological conditions, as well as for propagating these uncertainties consistently through to risk-based outcomes. This approach is demonstrated in the 'maximum' scenario, where we have examined the combined effect of 50% reduction in prescribing rates with optimal STW removal efficiencies. This shows that combining multiple interventions has the greatest effect, resulting in substantial reduction in risk level (Figure 6).

The identification of high-risk compounds (AZM, DFC, IBU, CLR) and high-risk locations provides a basis for prioritising mitigation measures. The above scenario analyses further demonstrate the scale of intervention required for risk reduction. For instance, large reductions in prescribing combined with substantial improvements in treatment efficiency may be needed to bring high-risk antibiotics below threshold exceedance levels. This should be further viewed in the context of demographic and prescribing trends in Scotland, with projected ageing population expected to increase the demand for health care and prescription medicines (Scottish Government, 2025). As a result, prescription rates are likely to increase or remain stable in coming decades, rather than decrease, making large reductions in prescribing a challenging management target in practice. While guidelines increasingly emphasise appropriate prescribing, demographic pressures could offset some of these gains. The reductions required to lower environmental concentrations for some pharmaceuticals below PNEC may therefore be difficult to achieve through prescribing policy alone and instead may necessitate enhanced wastewater treatment alongside other source control interventions. These insights can inform cost–benefit analyses of different management options. In the smaller headwater catchments with low dilution capacity, where high risk was predicted from smaller communal sewage treatment facilities (aka septic tanks), lower-cost solutions such as constructed wetlands may be effective (de Oliviera et al., 2020). In large STWs, specific treatment targeted at the removal of pharmaceutical compounds, such as the quaternary treatment envisaged in the revised EU Urban Wastewater Treatment Directive, may be needed (Council of the EU, 2024).

3.5 Utility and limitations of the BN framework

By implementing the pharmaceutical risk model into a BN, the input uncertainty can explicitly be accounted for and the resulting uncertainty quantified. This is a major advantage over most other

pharmaceutical modelling studies, where uncertainties are acknowledged but typically not quantified. As shown here and in previous studies, inputs such as prescription rates, excretion rates, WWTP removal efficiencies, river discharge estimates, and observational records are inherently uncertain, which significantly influence predicted concentrations and risks. The resulting probabilistic quantification of PNEC exceedance is also more in line with a standard risk assessment formulation (Mentzel et al., 2022; Welch et al., 2024).

Although this BN is functionally equivalent to a stochastic (Monte Carlo) mass balance model, it offers several advantages. It provides a transparent graphical representation of causal relationships between variables, facilitates communication of uncertainty, enables multiple uncertain datasets and expert-derived distributions to be combined consistently, and allows for both predictive and diagnostic inference. For example, the BN structure enabled straightforward evaluation of management scenarios, such as changes in prescribing or treatment efficiency, and to identify which pollution sources exert the greatest risk at specific locations. Moreover, this modular BN design is readily extendible: nodes representing CSOs, septic tanks, or in-stream attenuation can be added without re-coding the simulation framework. Additional management and future change scenarios can also be implemented relatively easily, following evolving stakeholder needs, data availability and scientific advances. Thus, while the present study demonstrates the BN in a relatively simple configuration, its value lies in the flexibility to evolve into a more comprehensive risk assessment tool.

The poorest model performance occurred where unaccounted sources (e.g. septic tanks, CSOs, veterinary use and diffuse sources) were likely to be present, hence pointing to clear priorities for future monitoring and model development. In-stream attenuation processes such as biodegradation, photolysis, hydrolysis, and sedimentation could also be incorporated in future model iterations, as done in Oldenkamp et al. (2018) and Wu et al. (2025). However, in-stream attenuation was assumed to be less influential in this study as the residence times in the river system are generally expected to be short relative to the typically slow and compound-specific degradation rates of many pharmaceuticals in surface waters (e.g. Bavumiragira et al., 2022). For example, Worrall et al. (2014) estimated a discharge-weighted median in-stream residence time of 26.7 h across 323 UK catchments. Residence times in the present study are therefore likely to be on the order of hours to a few days, particularly as the analysis focuses on transport between wastewater discharges and nearby monitoring points rather than across entire catchments.

Future work can also look to improve the spatial resolution of prescribing data (e.g. using a similar approach as in Jagadeesan et al., 2022) and include over the counter sales, where this data is available. Finally, risk assessments based on the single-compound PNEC exceedance approach must be interpreted cautiously, as PNECs also contain uncertainty (Mentzel et al., 2022), not accounted for in this study, and neglect mixture/additive effects and sub-lethal/selective pressures for anti-microbial resistance development (Tollefsen et al., 2025). Addressing this limitation is a clear future extension. Nonetheless, the BN framework provides a robust, transparent platform for evaluating intervention strategies under uncertainty and can support prioritisation of management actions at catchment scale.

4. Conclusions

We developed and applied a Bayesian Network to quantify catchment-scale pharmaceutical pollution risk from sewage treatment work discharges. By embedding a probabilistic mass-balance within a modular BN, we propagate uncertainty in prescribing, excretion, treatment removal and hydrology to produce distributions of monthly concentrations and exceedance probabilities for 16 pharmaceuticals at 20 monitoring locations. The model reproduces the major statistical features of the monitoring data for most compounds and locations, confirming that STW effluents are the dominant source in the catchment and that dilution (river flow) is an important driver of risk.

Scenario analyses show that climate-driven reductions in summer flows increase exceedance probabilities by mid- to late-century and that effective mitigation of the highest-risk compounds (e.g. azithromycin, diclofenac, ibuprofen, clarithromycin) will require either large reductions in prescribing, substantial improvements in STW removal performance or a combination of multiple system interventions. The BN's transparency and extensibility make it a practical decision-support tool, which can readily accommodate additional sources in future model development (CSOs, septic tanks, veterinary inputs). Furthermore, the model can be extended to mixture-based risk metrics relevant to understanding of ecological impacts and antimicrobial resistance. Future work should prioritise accounting for censored observations explicitly, improving the spatial allocation of prescribing (including OTC consumption), and integrating mixture effects to refine management recommendations.

Data and code availability

The BN model, the script for running the BN model using rSMILE, as well as the literature data on excretion and removal efficiency are available at:

https://github.com/madstroldborg/pharma-risk-BN-public

The repository includes processed input datasets for running the model and instructions for reproducing the results. However, licensed software dependencies and restricted raw datasets are excluded.

Author contributions

MT – formal analysis, data curation, investigation, methodology, software, validation, visualization, writing – original draft; MG – conceptualization, funding acquisition, methodology, software, project administration, resources, supervision, writing – review & editing; ZG – methodology, data curation, formal analysis, visualization, writing – review & editing; KA – methodology, data curation, formal analysis, writing – review & editing, CN – formal analysis, software, data curation, writing – review & editing; PT – data curation, writing – review & editing; ZZ – supervision, investigation, data acquisition, writing – review & editing; PC – investigation, data acquisition, writing – review & editing; AB – investigation, data acquisition, writing – review & editing; LM – supervision, writing – review & editing; ACF – formal analysis, methodology, writing – review & editing; LB - supervision, methodology, writing – review & editing; AT - funding acquisition, project administration, resources, supervision, writing – review & editing

Acknowledgements

This research was funded by the UKRI Freshwater Quality Program 'MOT4Rivers' project NE/X01620X/1 and the Scottish Government Strategic Research Program 2022-24 'Emerging Water Futures' project, and also supported by the Hydro Nation Chair Programme, funded by Scottish Water through the Scottish Funding Council. We thank Dr Alexis Walters for expert advice regarding wastewater treatment processes; Bess Homer for data and advice on Scottish Water wastewater treatment assets and interpretation of the UKCIP results; Dr Lydia Niemi from the Environmental Sustainability Institute, University of Highlands and Islands, for help with interpretation of ecotoxicological data.

Declaration of competing interest

The authors declare that they have no known competing financial interests or personal relationships that could have appeared to influence the work reported in this paper.

REFERENCES

1 Acker, S., Holloway, T., Harkey, M., 2025. Satellite detection of NO2 distributions using TROPOMI and TEMPO and comparison with ground-based concentration measurements, Atmos. Chem. Phys., 25, 8271–8288, https://doi.org/10.5194/acp-25-8271-2025.

2 Adams, K.J., Macleod, C.A.J., Metzger, M.J., Melville, N., Helliwell, R.C., Pritchard, J., Glendell, M., 2023. Developing a Bayesian network model for understanding river catchment resilience under future change scenarios. Hydrol. Earth Syst. Sci. 27,2205–2225. https://doi.org/10.5194/hess-27-2205-2023.

3 Austin, T.J., Comber, S., Forrester, E., Gardner, M., Price, O.R., Oldenkamp, R., Ragas, A.M.J., Hendriks A. J., 2021. The importance of over-the-counter-sales and product format in the environmental exposure assessment of active pharmaceutical ingredients. Science of The Total Environment, 752, 2021,141624, https://doi.org/10.1016/j.scitotenv.2020.141624.

4 aus der Beek, T., Weber, F.A., Bergmann, A., Hickmann, S., Ebert, I., Hein, A., Küster, A., 2016. Pharmaceuticals in the environment--Global occurrences and perspectives. Environ Toxicol Chem. 2016 Apr;35(4):823-35. doi: 10.1002/etc.3339.

5 Bavumiragira, J.P., Ge, J., Yin, H., 2022. Fate and transport of pharmaceuticals in water systems: A processes review, Science of The Total Environment, 823, 2022, 153635, https://doi.org/10.1016/j.scitotenv.2022.153635.

6 BayesFusion, 2025a. GeNIe 4.1. https://www.bayesfusion.com/, Accessed Dec 2025.

7 BayesFusion, 2025b. SMILE Engine, https://www.bayesfusion.com/smile, Accessed Dec 2025.

8 Boxall, A.B.A., Rudd, M.A., Brooks, B.W., Caldwell, D.J., Choi, K., Hickmann, S., et al., 2012. Pharmaceuticals and personal care products in the environment: what are the big questions? Environ Health Perspect. 2012 Sep;120(9):1221-9. doi: 10.1289/ehp.1104477.

9 Ceolotto, N., Dollamore, P., Hold, A., Balne, B., Jagadeesan, K.K., Standerwick, R., Robertson, M., Barden, R., Kasprzyk-Hordern, B., 2024. A new Wastewater-Based Epidemiology workflow to estimate community wide non-communicable disease prevalence using pharmaceutical proxy data. J. Hazard. Mater. 461, 132645.

10 Clara, M., Kreuzinger, N., Strenn, B., Gans, O., Kroiss, H., 2005. The solids retention time—a suitable design parameter to evaluate the capacity of wastewater treatment plants to remove micropollutants, Water Research, 39, Issue 1, 2005, 97-106,https://doi.org/10.1016/j.watres.2004.08.036.

11 Corrochano-Fraile, A. Wills, A. Brown, A and Beevers L. Projecting Climate Change Impacts on Scottish River Pollution. In review Climate Risk Management

12 Council of EU (2024, November 5). Urban wastewater: Council adopts new rules for more efficient treatment [Press release]. https://www.consilium.europa.eu/en/press/press-releases/2024/11/05/urban-wastewater-council-adopts-new-rules-for-more-efficient-treatment/
13 de Oliveira, M.; Atalla, A.A.; Frihling, B.E.F.; Cavalheri, P.S.; Migliolo, L.; Filho, F.J.C.M., 2019. Ibuprofen and Caffeine Removal in Vertical Flow and Free-Floating Macrophyte Constructed Wetlands with Heliconia Rostrata and Eichornia Crassipes. Chem. Eng. J. 2019, 373, 458–467.https://doi.org/10.1016/j.scitotenv.2019.135568
14 Environment Agency, 2016. Urban Waste Water Treatment Directive Treatment Plants [online dataset]. Available from: https://ckan.publishing.service.gov.uk/dataset/urban-waste-water-treatment-directive-treatment-plants [Accessed: 28 Nov 2025].
15 Gao, L., Maidment, I., Matthews, F.E., Robinson, L., Brayne, C., 2018. Medical Research Council Cognitive Function and Ageing Study. Medication usage change in older people (65+) in England over 20 years: findings from CFAS I and CFAS II. Age Ageing. 2018 Mar 1;47(2):220-225. doi: 10.1093/ageing/afx158. PMID: 29036509; PMCID: PMC6037294.
16 Glendell, M., Gagkas, Z., Stutter, M., Richards, S., Lilly, A., Vinten, A., Coull, M., 2022. A systems approach to modelling phosphorus pollution risk in Scottish rivers using a spatial Bayesian Belief Network helps targeting effective mitigation measures. Front. Environ. Sci. 10.
17 Holton, E., Sims, N., Jagadeesan, K., Standerwick, R., Kasprzyk-Hordern, B., 2022. Quantifying community-wide antimicrobials usage via wastewater-based epidemiology. J. Hazard. Mater. 436, 129001.
18 Hyun, S, Mishra, A, Follett, CL, Jonsson, B, Kulk, G, Forget, G, Racault, MF, Jackson, T, Dutkiewicz, S, Müller, CL, Bien, J. , 2022. Ocean mover's distance: using optimal transport for analysing oceanographic data. Proc Math Phys Eng Sci. 2022 Jun;478(2262):20210875. doi: 10.1098/rspa.2021.0875. Epub 2022 Jun 22. PMID: 35756877; PMCID: PMC9215217.
19 Jagadeesan, K.K., Grant J., Griffin S., Barden., R, Kasprzyk-Hordern., B. PrAna: an R package to calculate and visualize England NHS primary care prescribing data. BMC Med Inform Decis Mak. 2022 Jan 6;22(1):5. doi: 10.1186/s12911-021-01727-z. PMID: 34991567; PMCID: PMC8734375.
20 Jagadeesan, K. K., Proctor, K., Standerwick, R., Barden, R., & Kasprzyk-Hordern, B., 2025. Predicting pharmaceutical concentrations and assessing risks in the aquatic environment using PERK: A case study of a catchment area in South-West England. Water Research, 268, Article 122643. https://doi.org/10.1016/j.watres.2024.122643
21 Kaikkonen, L, Parviainen, T, Rahikainen, M, Uusitalo, L, Lehikoinen, A., 2021. Bayesian Networks in Environmental Risk Assessment: A Review. Integr Environ Assess Manag. 2021 Jan;17(1):62-78. doi: 10.1002/ieam.4332.
22 Kannan, A., Sims, N., Hold, A.J., Jagadeesan, K., Standerwick, R., Barden, R., Kasprzyk-Hordern, B., 2023. The burden of city's pain treatment – A longitudinal one year study of two cities via wastewater-based epidemiology. Water Res. 229, 119391.
23 Knox, C, Wilson, M, Klinger, CM, et al., 2024. DrugBank 6.0: the DrugBank Knowledgebase for 2024. Nucleic Acids Res. 2024 Jan 5;52(D1):D1265-D1275. doi: 10.1093/nar/gkad976 . PMID: 37953279 ; PMCID: PMC10767804.
24 Korb, K.B., Nicholson, A.E., 2003. Bayesian Artificial Intelligence. CRC Press, USA
25 Menéndez, M. L., Pardo, J. A., Pardo, L., and Pardo, M. C., 1997. The Jensen-Shannon divergence, J. Frankl. Inst., 334, 307–318, https://doi.org/10.1016/S0016-0032(96)00063-4.
26 Mentzel, S., Grung, M., Tollefsen, K. E., Stenrød, M., Petersen, K., & Moe, S. J., 2022. Development of a Bayesian network for probabilistic risk assessment of pesticides. Integrated Environmental Assessment and Management, 18(4), 1072–1087. https://doi.org/10.1002/ieam.4533
27 Moe, SJ, Carriger, JF, Glendell, M., 2021.Increased Use of Bayesian Network Models Has Improved Environmental Risk Assessments. Integr Environ Assess Manag. 2021 Jan;17(1):53-61. doi: 10.1002/ieam.4369.

28 Negri, C., Schurch, N., Wade, A.J., Mellander, P.-E., Stutter, M., Bowes, M.J., Mzyece, C.C., Glendell, M., 2024. Transferability of a Bayesian Belief Network across diverse agricultural catchments using high-frequency hydrochemistry and land management data. Science of The Total Environment 949, 174926.
29 Niemi, L, Arakawa, N, Glendell, M, Gagkas, Z, Gibb, S, Anderson, C, Pfleger, S., 2024. Co-developing frameworks towards environmentally directed pharmaceutical prescribing in Scotland - A mixed methods study. Sci Total Environ. 2024 Dec 10;955:176929. doi: 10.1016/j.scitotenv.2024.176929. Epub 2024 Oct 31. PMID: 39461523.
30 NORMAN, 2025. NORMAN Ecotoxicology Database. https://www.norman-network.com/nds/ecotox/ (accessed 23-09-2025)
31 OHBP, 2025. Pharmaceuticals in the Water Environment. One Health Breakthrough Partnership (OHBP). https://informatics.sepa.org.uk/EnvironmentalPharmaceuticals/ (accessed 2025-
32 Oldenkamp, R.; Hoeks, S.; Čengić, M.; Barbarossa, V.; Burns, E. E.; Boxall, A. B. A.; Ragas, A. M. J., 2018. A High-Resolution Spatial Model to Predict Exposure to Pharmaceuticals in European Surface Waters: ePiE. Environ. Sci. Technol. 2018, 52, 12494– 12503, https://doi.org/10.1021/acs.est.8b03862.
33 Pearl, J. 2014. Graphical models for probabilistic and causal reasoning. In: A. Tucker, T. Gonzalez, H. Topi, J. Diaz-Herrera (Eds.) Computing Handbook (Renamed), Third Edition, Volume 1, Intelligent Systems section, Chapman and Hall/CRC, 2014.
34 Petrie B., Barden R., Kasprzyk-Hordern B., 2015. A review on emerging contaminants in wastewaters and the environment: Current knowledge, understudied areas and recommendations for future monitoring, Water Research, Volume 72, 2015,https://doi.org/10.1016/j.watres.2014.08.053.
35 Pham, H.V., Sperotto, A., Furlan, E., Torresan, S., Marcomini, A., Critto, A., 2021. Integrating Bayesian Networks into ecosystem services assessment to support water management at the river basin scale. Ecosyst. Serv. 50, 101300. https://doi.org/10.1016/j.ecoser.2021.101300
36 PHS, 2025. Prescribing Information System, Public Health Scotland, 2025. https://www.opendata.nhs.scot/dataset (accessed September 2025-09-23).
37 Ramage, S., Camacho-Muñoz, D., Petrie, B., 2019. Enantioselective LC-MS/MS for anthropogenic markers of septic tank discharge. Chemosphere, 219, 2019, 191-201, https://doi.org/10.1016/j.chemosphere.2018.12.007.
38 Ren, H., Zhang, Z., Gong, Q., 2025. Estimation of Shannon entropy of the inverse exponential Rayleigh model under progressively Type-Ⅱ censored test. AIMS Mathematics, 2025, 10(4): 9378-9414. doi: 10.3934/math.2025434.
39 Rowland, C.S., Marston, C., O'Neil, A.W., 2025. Land Cover Map 2024 (25m rasterised land parcels, GB). NERC EDS Environmental Information Data Centre. https://doi.org/10.5285/0e3ab6f8-4a20-4a60-a804-e144fb0bde39
40 The Scottish Government, 2025. Population Health Framework: evidence paper. June 17, 2025. ISBN: 9781836915843. https://www.gov.scot/publications/population-health-framework-evidence-paper/ [accessed 28/1/2026]
41 SEPA 2011, River Almond Catchment Profile, Scottish Environmental Protection Agency (SEPA) website, published September 2011, https://www.sepa.org.uk/media/74998/doc-14-river-almond.pdf,
42 Soch, J. (2020). Proof: Method of moments for beta-distributed data. The Book of Statistical Proofs (Version 2023), Proof #28. URL: https://statproofbook.github.io/P/beta-mome; DOI: 10.5281/zenodo.4305949.
43 Ternes, T.A., 1998. Occurrence of drugs in German sewage treatment plants and rivers. Water Res 1998;32:3245–60.
44 Ternes, T.A., Kreckel, P., Mueller, J., 1999. Behaviour and occurrence of estrogens in municipal sewage treatment plants e II. aerobic batch experiments with activated sludge. Sci. Total Environ. 225, 91-99.
45 Thornber, K., Adshead, F., Balayannis, A., et al., 2022. First, do no harm: time for a systems approach to address the problem of health-care-derived pharmaceutical pollution. The Lancet Planetary Health, Volume 6, Issue 12, e935 - e937. https://doi.org/10.1016/S2542-5196(22)00309-6

46 Thornber, K., Bentham, M., Pfleger, S., et al., 2026. Pharmaceutical pollution from health care: a systems-based strategy for mitigating risks to public and environmental health. The Lancet Planetary Health, Volume 10, Issue 1, 101404. https://doi.org/10.1016/j.lanplh.2025.101404.

47 Tollefsen, K.E., Moe, S.J., Meland S., Mentzel S., Grung M., Welch S., Rødland E.S., 2025. Cumulative and Probabilistic Risk Assessment of Enhanced Nature-based Treatment System Pilots. MULTISOURCE Deliverable 2.3. https://multisource.eu/storage/2025/11/D2.3-%E2%80%93-Cumulative-and-Probabilistic-Risk-Assessment-of-Enhanced-Nature-based-Treatment-System-Pilots.pdf

48 Troldborg, M., Gagkas, Z., Vinten, A., Lilly, A., Glendell, M., 2022. Probabilistic modelling of the inherent field-level pesticide pollution risk in a small drinking water catchment using spatial Bayesian belief networks. 2022. Hydrol Earth Syst Sci. https://doi.org/10.5194/hess-2021-477.

49 Villani, C., 2009. The Wasserstein distances. In: Optimal Transport: Old and new. Grundlehren der mathematischen Wissenschaften, vol 338. Springer, Berlin, Heidelberg. https://doi.org/10.1007/978-3-540-71050-9_6.

50 VMD, 2025. Product Information Database https://www.vmd.defra.gov.uk/ProductInformationDatabase (accessed 14/11/2025).

51 Welch, S.A., Grung, M., Madsen, A. L., Moe, S.J., 2024. Development of a probabilistic risk model for pharmaceuticals in the environment under population and wastewater treatment scenarios, Integrated Environmental Assessment and Management, Volume 20, Issue 5, 1 September 2024, Pages 1715–1735, https://doi.org/10.1002/ieam.4939

52 Wick, A., Fink, G., Joss, A., Siegrist, H., Ternes, T.A., 2009. Fate of beta blockers and psycho-active drugs in conventional wastewater treatment. Water Research 43, 1060-1074.

53 Wilkinson, J.L., Boxall, A.B.A., Kolpin, D.W., Leung, K.M.Y., Lai, R.W.S., Galbán-Malagón, C., et al., 2022. Pharmaceutical pollution of the world's rivers, Proc. Natl. Acad. Sci. U.S.A. 119 (8) e2113947119, https://doi.org/10.1073/pnas.2113947119.

54 Worrall, F., Howden, N.J.K. , Burt, T.P., 2014. A method of estimating in-stream residence time of water in rivers, Journal of Hydrology, 512, 2014, 274-284, https://doi.org/10.1016/j.jhydrol.2014.02.050.

55 Wu, S., Helm, B., Teran-Velasquez, G., Krebs, P., Kumar, R., 2025. Spatially and Seasonally Resolved Predictions Reveal Widespread Ecotoxicological Risk from Pharmaceutical Mixtures in German (Saxon) Rivers. Environmental Science & Technology 2025 59 (33), 17722-17734, DOI: 10.1021/acs.est.5c01639

56 UKWIR, 2025. Chemical Investigation Programme - Data Access Portal. https://ukwir.org/water-chemicals-investigation-programme (accessed September 2025-09-23).

57 Umwelt Bundesamt, "Database- Pharmaceuticals in the environment" Umwelt Bundesamt, 2021. https://www.umweltbundesamt.de/en/database-pharmaceuticals-in-the-environment-0 (accessed September 2025).

58 Zorita, S., Mårtensson, L., Mathiasson, L., 2009. Occurrence and removal of pharmaceuticals in a municipal sewage treatment system in the south of Sweden, Science of The Total Environment,407 (8),2009, 2760-2770, https://doi.org/10.1016/j.scitotenv.2008.12.030.

Non-peer reviewed preprint submitted to EarthArXiv

Supporting information

Probabilistic modelling of pharmaceutical pollution risk from sewage treatment work discharges using a Bayesian Network: application to a Scottish river catchment

Mads Troldborg[1*], Miriam Glendell[2*], Zisis Gagkas[2], Kerr Adams[2], Camilla Negri[2], Phil Taylor[4], Zulin Zhang[2], Pat Cooper[2], Alison Brown[3], Linda May[4], Ana Corrochano-Fraile[5], Lindsay Beevers[5], Andrew Tyler[3]

[1] The James Hutton Institute, Information and Computational Sciences Department, Invergowrie, Dundee, United Kingdom.
[2] The James Hutton Institute, Environmental and Biochemical Sciences Department, Craigiebuckler, Aberdeen, United Kingdom.
[3] University of Stirling, Stirling, United Kingdom.
[4] UK Centre for Ecology & Hydrology. Bush Estate, Penicuik, Midlothian, United Kingdom.
[5] Institute of Infrastructure and Environment, School of Engineering, University of Edinburgh, Edinburgh United Kingdom.

* Corresponding authors. mads.troldborg@hutton.ac.uk miriam.glendell@hutton.ac.uk

S1. Bayesian network nodes and parameterisation

Table S1.1: Summary of BN nodes.

Node (symbol)	States/parameterisation	Description
Month	Jan, Feb, Mar, Apr, May, Jun, Jul, Aug, Sep, Oct, Nov, Dec	
Pharmaceutical	See Table 1	The 16 target pharmaceuticals.
Total PE (PE_{tot})	Deterministic (see details in SI 2).	Total population (people equivalent) served by the sewage treatment works (STWs) upstream of a given monitoring point. Processed STW data available in accompanying GitHub repository (see Data and code availability)
Wastewater treatment category	P SAS SB TA TB	See Table S2.5. Processed STW data available in accompanying GitHub repository (see Data and code availability)
Standardised mass prescribed (M_p)	Equation	Monthly pharmaceutical mass prescribed per person (g month^{-1} 1000 people^{-1}). Monthly prescribing data from 2019-2024 within NHS Lothian have been downloaded from Public Health Scotland for each target pharmaceutical. Normal distributions have been fitted to the monthly prescribing data for each pharmaceutical. See details in S2.2. Processed prescription data available in accompanying GitHub repository (see Data and code availability)
Excretion rate (ER_p)	Equation	Fraction (between 0 and 1) of pharmaceutical p excreted by humans following administration. Beta probability distributions have been fitted to excretion data collated from literature for each pharmaceutical. See details in S2.3. Collated excretion data from literature is available in accompanying GitHub repository (see Data and code availability)
Removal efficiency ($RR_{ef,p}$)	Eq. 4	Fraction (between 0 and 1) of pharmaceutical removed during wastewater treatment. See details in S2.4. Collated removal efficiency data from literature is available in accompanying GitHub repository (see Data and code availability)
Predicted no-effect concentration ($PNEC_p$)	Deterministic (see Table 1)	Predicted no-effect concentration (PNEC) (µg l^{-1}) of pharmaceutical p. PNECs have been collated from the NORMAN Ecotoxicological database.
Influent load $\left(L_p^{infl}\right)$	Equation: M_p x PE_{tot} x ER_p/1e6	Total mass of pharmaceutical p entering the STWs upstream the monitoring point (kg month^{-1}). Intermediate node.
Effluent load $\left(L_p^{effl}\right)$	Equation: $L_p^{infl} x RR_{ef,p}$	Total mass of pharmaceutical p discharged with the effluent from the STWs upstream of the monitoring point (kg month^{-1}). Intermediate node.
Daily discharge (Q_j)	Equation	Daily river discharge (m^3 s^{-1}) at monitoring point j. Daily river discharge at each monitoring point has been simulated from 2015-2024 using a calibrated SWAT model for the catchment. For each

		monitoring point, log-normal distributions have been fitted to the daily river flows by month. Processed flow data available in accompanying GitHub repository (see Data and code availability)
Predicted concentration ($C_{p,j}$)	Equation (Eq. 4): $\frac{L_{p,i}^{effl} \times 1e6}{Q_j \times 86400 \times 30}$	Predicted concentration (µg l^{-1}) og pharmaceutical p at monitoring point j.
Predicted log risk ratio (PLRR)	Equation (Eq. 3): $Log10(C_{p,j}/PNEC_p)$	
PNEC exceedance probability	Above Below	Above: Probability of PLRR > 0 Below: Probability of PLRR < 0
Prescription scenario	baseline reduced_10pct reduced_50pct	Management node to explore the effect of reducing prescribing rates. The node acts as a multiplier with mass prescribed (baseline=1; reduced_10pct=0.9; reduced_50pct=0.5)
Treatment scenario	baseline optimal	Management node to explore effect of improved wastewater treatment removal efficiencies. When "optimal", the removal efficiency probability distributions for each pharmaceutical-treatment category combination are fixed at their respective 90^{th} percentile.

S2. Data sources

S2.1 STW information

Table S2.1: Overview of the sewage treatment works in the River Almond catchment, the treatment processes employed, and population served (Scottish Water, personal communication, January 30, 2024).

STW name	**WWTW process**	**PE**
East Calder	Activated sludge (tertiary)	117522
Newbridge	Activated sludge (tertiary)	30972
Blackburn	Biological (tertiary)	21681
Whitburn	Activated sludge (tertiary)	14220
Livingston	Biological (tertiary)	5597
Fauldhouse	Biological (tertiary)	5295
Winchburgh	Biological (tertiary)	4578
Harthill	Activated sludge (tertiary)	3945
Addiewell	Septic Tank (primary)	98
Camps	Septic Tank (primary)	95
Ritchie camps	Biological (secondary)	62
Linburn	Biological (secondary)	52
Old Bathgate Road	Septic Tank (primary)	9

S2.2 Prescribing rates

Monthly standardised masses prescribed (g/1000 people) between 2019–2024 were derived from the Public Health Scotland Prescribing Information System (PIS) database (PHS, 2025). PIS holds 100% of NHS Scotland prescriptions dispensed within the community and claimed for payment by a

pharmacy contractor (i.e. general practices (GPs), community pharmacies, dental clinics and hospitals). PIS includes monthly datasets containing the number of prescribed BNF (British National Formulary) items and associated quantities by GP practice (given by unique GP codes). An item is an individual product dispensed (e.g. a pack of 100 aspirin tablets of 300mg), whereas the quantity is the quantity contained within the item (e.g. 100 tablets). Each item is given by a unique 15-digit British National Formulary (BNF) Item code in which the first seven digits are allocated according to the categories in the BNF, and the last 8 digits represent the medicinal product, form, strength and the link to the generic equivalent product.

To extract the prescription data, all the BNF codes that apply to each of the target pharmaceuticals (Table 1) were first identified via https://openprescribing.net/chemical/ (accessed 14/10/2025). Table S2.2 shows a list of the selected compounds and their associated BNF codes (first 9 digits). Note, it was decided to exclude any products used for Eye (chapter 11), Ear, Nose and Oropharynx (chapter 12), Skin (chapter 13) and any gel products.

Table S2.2: Selected compounds, their BNF codes and categorisation. Codes highlighted in bold are the one that were ultimately included in the analysis here. CS: Cardiovascular System; CNS: Central Nervous System. ENT: Ear, Nose and Oropharynx; UTD: Urinary-Tract Disorders.

Compound	**BNF code**	**BNF chapter/section/paragraph**
Azithromycin	0501050A0	Infection/Antibacterial/Macrolide
Bezafibrate	0212000D0	CS/Lipid-regulating drugs/NA
Carbamazepine	0408010C0	CNS/Antiepileptic drugs/Control of epilepsy
Ciprofloxacin	0501120L0	Infection/Antibacterial/Quinolones
Clarithromycin	0501050B0	Infection/Antibacterial/Macrolide
Diclofenac	1001010AG 1001010C0 1003020AF 1003020U0	Musculoskeletal/Drugs for rheumatic diseases & gout/NSAIDs. Musculoskeletal/Drugs for soft-tissue disorders & pain relief/Rubefacients & other NSAIDs.
Erythromycin	0501050C0 0501050H0 0501050K0 0501050N0	Infection/Antibacterial/Macrolide
Hydrochlorothiazide	0202010L0 0202040C0 0202040H0 0205051G0 0205052AC 0205052Y0	CS/Diuretics/Thiazides and related diuretics CS/Diuretics/Potassium sparing diuretics & compounds CS/Diuretics/Potassium sparing diuretics & compounds CS/Diuretics/ Renin-angiotensin system drugs CS/Diuretics/ Renin-angiotensin system drugs CS/Diuretics/ Renin-angiotensin system drugs
Ibuprofen	0309020AA 0407010AD 0701011F0 1001010AD 1001010AM 1001010AP 1001010J0 1003020P0	Respiratory System/Cough prepn/Expectorant & demulcent cough prepn. CNS/Analgesics, paragraph/Non-opioid analgesics & compound prepn. Obs, Gynae, UTD / Drugs used in obstetrics/Prostaglandins & oxytocics. Musculoskeletal /Drugs used in rheumatic diseases & gout/NSAIDs. Musculoskeletal/Drugs for soft-tissue disorders & pain relief/ Rubefacients & others NSAIDs.
Naproxen	100101070 1001010P0	Musculoskeletal /Drugs used in rheumatic diseases & gout/NSAIDs
Paracetamol	040701020 0407010AB 0407010AD 0407010F0 0407010H0 0407010N0	CNS/Analgesics, paragraph/Non-opioid analgesics & compound prepn.

	0407010Q0 0407010U0 0407010X0	
Ranitidine	0103010S0 0103010T0	Gastro-Intestinal System/Antisecretory & mucosal protectants/H2-receptor antagonists
Sulfadiazine	0501080J0	Infections/Antibacterial/Sulfonamides and trimethoprim.
Sulfamethoxazole	0501080D0	Infection/Antibacterial/ Sulfonamides and trimethoprim
Tramadol	040702040	CNS/ Analgesics/Opioid analgesics
Trimethoprim	0501080D0 0501080W0	Infection/Antibacterial/ Sulfonamides and trimethoprim

All the unique BNF items associated with the chosen BNF codes were extracted and examined to determine the strength of pharmaceutical compound in the given item. By multiplying the strength of the item with the quantity prescribed by the given GP in the given month, the total monthly pharmaceutical mass prescribed (via this item) was calculated for the given GP. The total monthly pharmaceutical mass was then calculated by summing the monthly masses from all the relevant BNF items.

The calculated total monthly pharmaceutical masses by GP were aggregated spatially within, respectively, the study catchment and the health boards; and the monthly standardised prescription rates (g/person) was subsequently calculated by dividing by, respectively, the combined list size of the GPs within the study catchment or the health board population. For the former, it was necessary to geo-reference the GPs. The GP addresses and list sizes are available from: https://www.opendata.nhs.scot/dataset/gp-practice-contact-details-and-list-sizes (accessed 14/10/2025)

It should be noted that the database also includes prescriptions that do not originate from GPs and where the exact location of origin cannot be determined; this includes e.g. hospitals, dentist surgeries, and non-regular prescribing practices such as out-of-hours and urgent care services. The prescribing contribution from these are only available as aggregated numbers at health board level.

Mean and standard deviation of the standardised prescription rates were calculated by month and health board and used as input for the BN model, assuming the monthly prescription rates to follow a normal distribution. The study catchment is located in NHS Lothian, hence the summarised prescribing data for this health board was used as input for the final BN model.

Figure S2.1 and Figure S2.2 shows, respectively, histograms and timeseries of the monthly standardised prescribed mass of the 16 target pharmaceutical in NHS Lothian between 2019 and 2024. Table S2.3 shows the calculated monthly mean and standard deviation of the standardised prescribed masses in Lothian. Paracetamol is by far the compound that is prescribed at the highest rate (around 4000 g/1000 people/month) followed by naproxen (approx. 150 g/1000 people/month) and ibuprofen (approx. 100 g/1000 people/month). Note that both paracetamol and ibuprofen can be bought over the counter (OTC), so the actual consumption rates of these drugs are likely to be significantly higher. For example, Austin et al. (2021) estimated OTC sales of ibuprofen to make up 76% of the total mass of ibuprofen sold or prescribed in the UK. Ranitidine was also previously available over the counter in the UK, but all ranitidine products were banned from use in 2019, and ranitidine has therefore seen a dramatic decrease in prescription rates. Overall, the monthly prescription rates of the different pharmaceuticals show fairly limited seasonal variation (Table S2.3). Note that the full five-year period was used to calculate monthly average prescription rates and any increasing or decreasing trends, where significant or not, were not accounted for or used in predicting future usage.

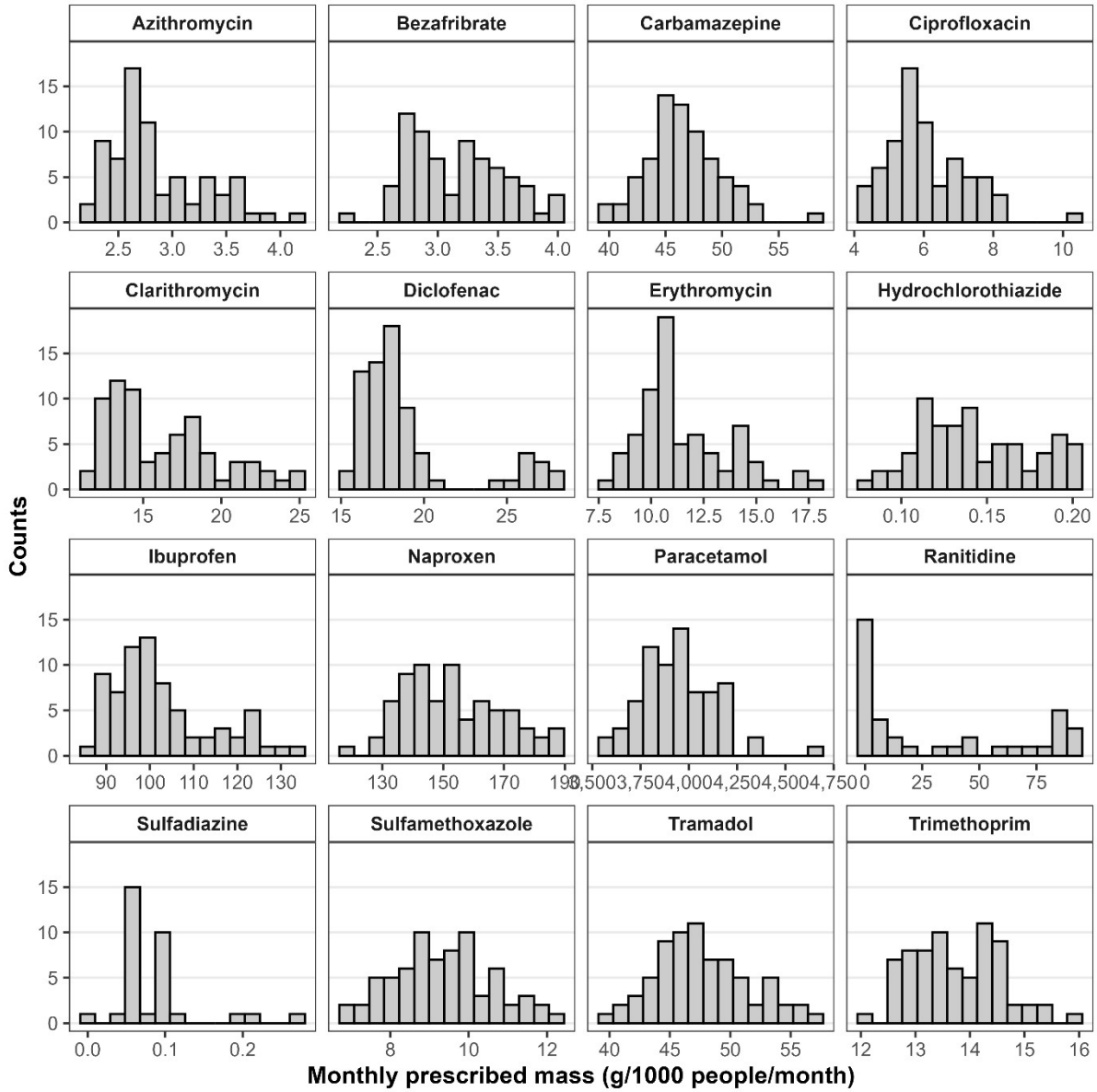

Figure S2.1: Histograms of standardised monthly prescription rates between 2019-2024 in NHS Lothian by pharmaceuticals.

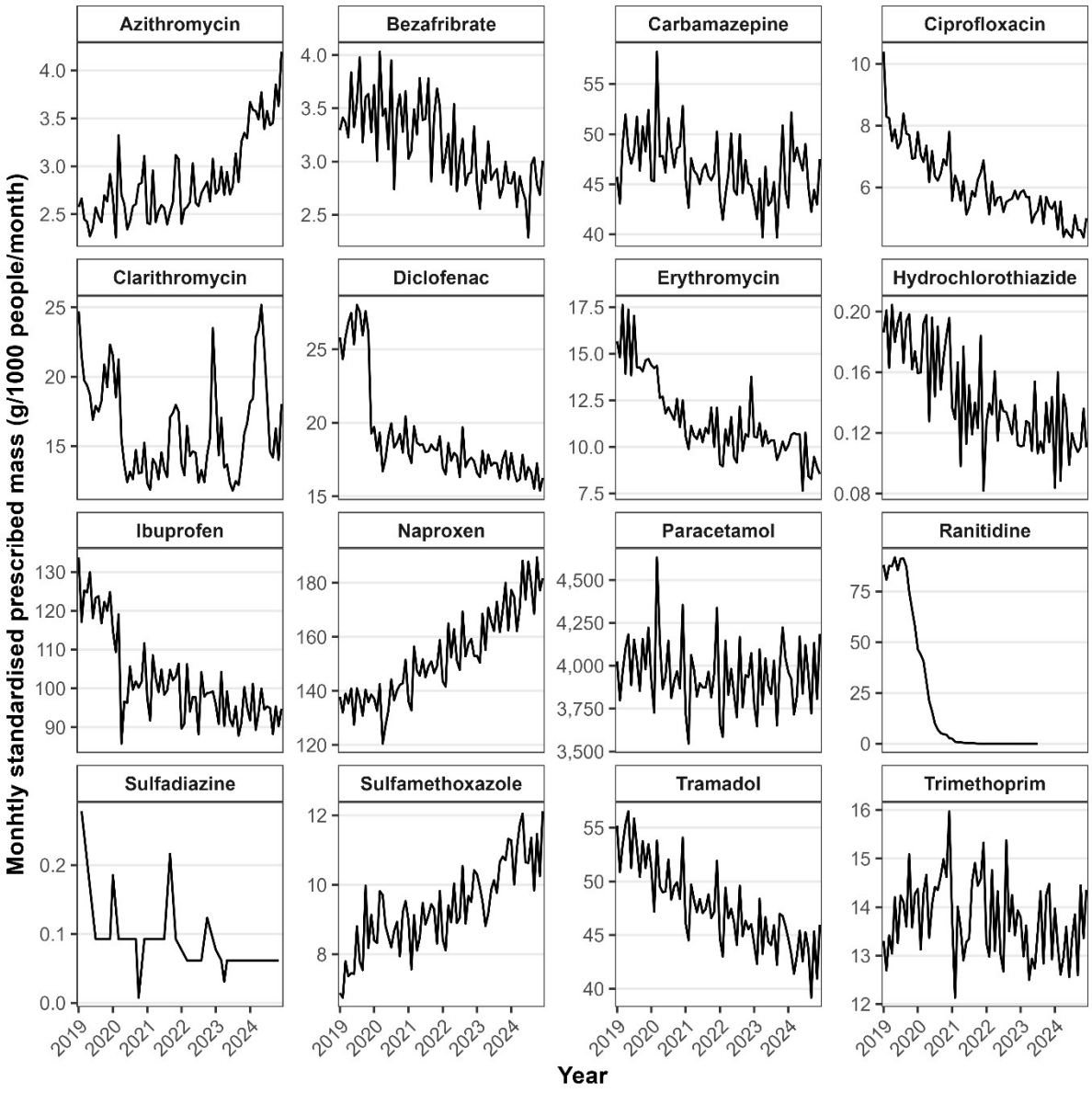

Figure S2.2: Monthly prescription time series in NHS Lothian between 2019-2024 by pharmaceutical.

Table S2.3. Monthly mean (standard deviation) of the standardised prescription rates (g/1000 people/month) for the target pharmaceuticals by month in NHS Lothian.

	Jan	**Feb**	**Mar**	**Apr**	**May**	**Jun**	**Jul**	**Aug**	**Sep**	**Oct**	**Nov**	**Dec**
Azithromycin	2.8 (0.5)	2.7 (0.5)	3 (0.4)	2.7 (0.4)	2.9 (0.5)	2.7 (0.4)	2.8 (0.4)	2.8 (0.4)	2.7 (0.2)	2.9 (0.3)	2.9 (0.3)	3.1 (0.1)
Bezafibrate	3.1 (0.4)	3.0 (0.3)	3.3 (0.5)	3.0 (0.3)	3.5 (0.4)	3.0 (0.3)	3.2 (0.6)	3.3 (0.5)	3 (0.3)	3.3 (0.4)	3.3 (0.4)	3.3 (0.3)
Carbamazepine	44.6 (1.3)	44.6 (4.1)	48.9 (5.1)	47.0 (4.1)	48.0 (1.4)	45.6 (1.5)	47.3 (3.2)	48.1 (2.8)	44.8 (2.9)	47.7 (2.4)	48.1 (2.3)	49.2 (4.1)
Ciprofloxacin	6.9 (2.0)	6.3 (1.3)	6.5 (1)	6.0 (1.2)	5.9 (1.2)	5.8 (1.2)	5.7 (1.1)	6.2 (1.2)	6.1 (1.1)	6.5 (0.9)	6.3 (0.6)	6.5 (1.0)
Clarithromycin	18.3 (4.7)	16.3 (3.8)	18.7 (3.3)	16.7 (4)	16.5 (4.8)	15.5 (3.7)	14.6 (2.9)	14.0 (2.0)	15.0 (2.7)	16.0 (3.3)	16.5 (2.4)	19.1 (3.7)
Diclofenac	19.3 (3.5)	18.3 (3.1)	19.7 (3.3)	18.8 (4.1)	19.6 (3.9)	19.1 (3.4)	19.5 (4.4)	19.7 (4.1)	19.4 (3.9)	20.1 (4.3)	19.7 (3.7)	18.6 (1.7)
Erythromycin	11.8 (2.7)	11.6 (2.4)	12.7 (2.8)	11.4 (1.6)	12.3 (2.7)	10.7 (2.1)	11.7 (2.8)	11.4 (2.0)	11.2 (2.0)	11.9 (1.7)	11.4 (1.9)	12.6 (1.9)
Hydrochlorothiazide	0.1 (0.04)	0.2 (0.03)	0.2 (0.04)	0.2 (0.04)	0.1 (0.03)	0.2 (0.04)	0.1 (0.03)	0.1 (0.03)	0.1 (0.03)	0.2 (0.03)	0.2 (0.03)	0.1 (0.1)
Ibuprofen	104 (17)	101 (11)	109 (13)	99 (14)	104 (13)	101 (10)	101 (13)	103 (11)	102 (11)	104 (12)	105 (9)	108 (12)
Naproxen	148 (16)	145 (17)	156 (12)	148 (17)	157 (22)	151 (18)	156 (18)	158 (19)	148 (12)	152 (12)	154 (17)	154 (9)
Paracetamol	3864 (145)	3723 (142)	4123 (303)	3961 (157)	4031 (152)	3899 (40)	3992 (194)	3997 (128)	3848 (125)	3996 (122)	4013 (137)	4229 (146)
Ranitidine	34.4 (41.9)	42.0 (40.1)	43.2 (43.6)	39.8 (44.2)	38.0 (48.1)	34.1 (45.5)	25.4 (44.3)	33 (50.9)	31 (49)	26.6 (42.1)	23.6 (37.0)	20.3 (32.8)
Sulfadiazine	0.1 (0.1)	0.0 (0.0)	0.1 (0.02)	0.0 (0.0)	0.1 (0.02)	0.1 (0.02)	0.1 (0.02)	0.0 (0.0)	0.1 (0.1)	0.1 (0.1)	0.1 (0.02)	0.1 (0)
Sulfamethoxazole	9.1 (1.6)	8.5 (1.3)	9.5 (1.1)	9.2 (1.5)	9.4 (1.6)	9.2 (1.1)	9.3 (0.9)	9.6 (1.3)	9.1 (1.1)	9.6 (1.1)	9.2 (1.0)	10.1 (0.9)
Tramadol	47.9 (4.6)	45.4 (3.3)	49.6 (4.5)	47.9 (4.6)	48.9 (4.0)	47.2 (3.2)	48.3 (4.9)	48.3 (3.3)	47.4 (3.5)	49 (3.2)	48.1 (2.2)	50.5 (4.1)
Trimethoprim	13.8 (0.4)	12.9 (0.4)	13.9 (0.8)	13.4 (0.8)	13.6 (0.6)	13.2 (0.5)	13.7 (0.7)	14.5 (0.5)	14 (0.9)	14.7 (0.4)	14.2 (0.6)	14.6 (1.2)

S2.3 Excretion rates

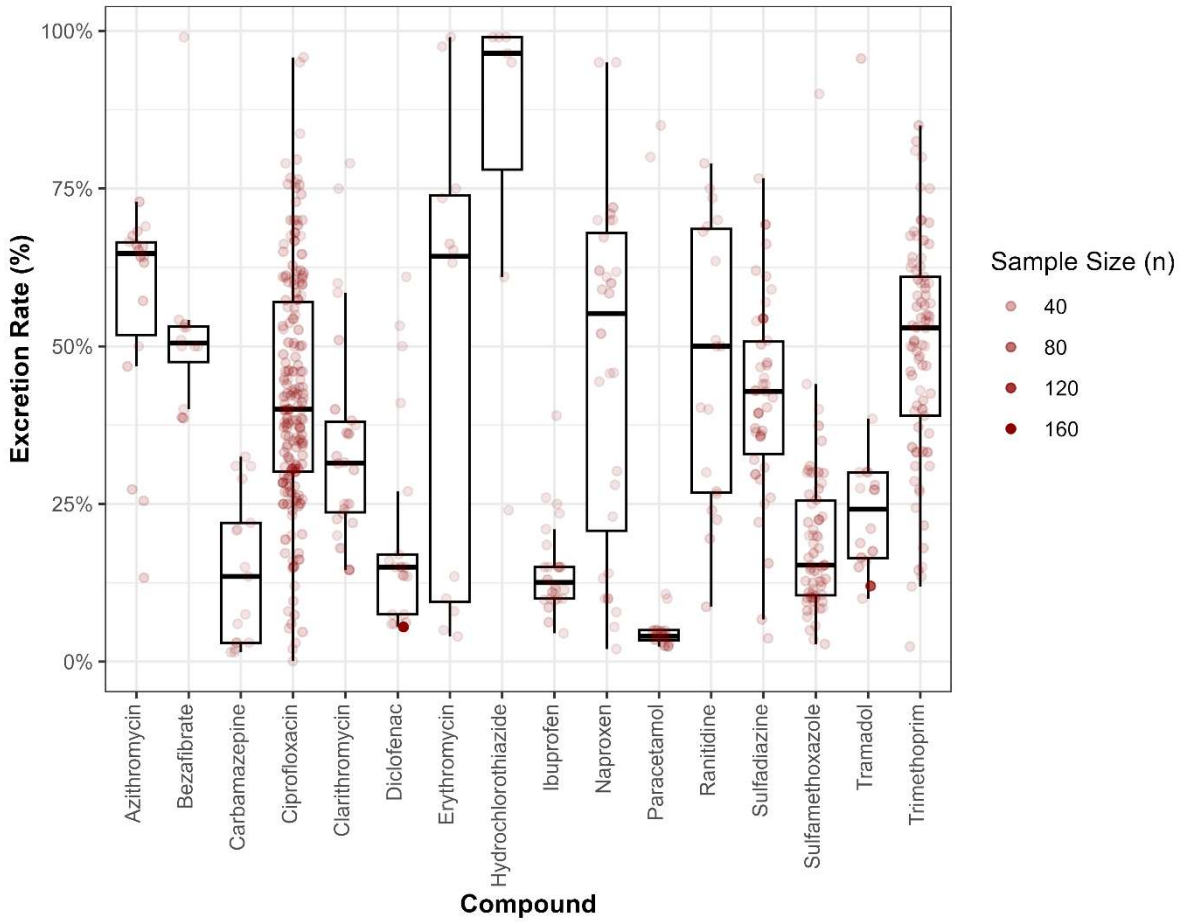

Figure S2.3: Boxplots of human excretion rates collated from for each of the 16 target pharmaceuticals (see 'Data and code availability'). Each point represents a study and is shaded based on number of observations/subjects used in the study.

S2.4 STW removal efficiencies

In the literature, the removal efficiencies are typically estimated by monitoring paired concentrations of pharmaceutical in the influent (raw sewage) and treated effluent from STWs and simply calculating the percent change in concentrations. This approach has a number of limitations (Petrie et al., 2015): (i) The hydraulic and solid retention times during treatment are (usually) not accounted for, so the influent and effluent data taken at any point in time can in principle not be directly paired and compared. It is likely that the influent concentrations are much more variable during the day/over shorter time periods compared to the effluent concentrations from a treatment plant, where mixing and stirring in a number of tanks takes place. However, it should be noted that most studies in the literature appear to use (24-hr) composite sampling, rather than e.g. spot samples, to mitigate the effect of this temporal variability in concentrations; (ii) The removal rate is estimated on a concentration basis and does not account for potential differences in influent and effluent flow rates or for partitioning of pharmaceuticals to solid matter during wastewater treatment. If the flow rates are known, then the removal can be estimated on a mass discharge basis, which would be a more accurate reflection of the actual removal. Only a limited number of studies appear to have investigated and accounted for differences in flow rates and the partitioning of the pharmaceuticals into soluble and solid/sludge phases when estimating removal rates.

The above limitations can perhaps to some extent explain why the removal efficiencies of certain pharmaceuticals have often been estimated to be negative (i.e., when concentrations in effluent are higher than in influent). Negative removal rates are typically attributed to deconjugation of metabolites into their parent compounds or analytical and sampling variability (Ternes et al. 1999; Wick et al., 2009). Several pharmaceuticals are known to be excreted as (glucuronide) conjugates. For example, the major metabolite in humans of carbamazepine is 10, 11 epoxy-carbamazepine, which is hydrolysed further and are excreted principally as glucuronides (Ternes, 1998). These glucuronide-conjugates can presumably be cleaved in sewage and during sewage treatment and thus increase the environmental concentrations (Ternes, 1998), although the process is still not well-understood.

Although negative apparent removal efficiencies are frequently reported and attributed to deconjugation of metabolites, allowing negative removal efficiencies in a forward mass-balance model would imply net generation of parent compound from mass not represented at the excretion stage. To maintain mass consistency, removal efficiencies were constrained to [0,1]. Under this formulation, estimated effluent loads represent the discharge of parent compound excreted as parent, and may underestimate total parent discharge where reconversion from metabolites is significant.

Table S2.4. Classification of STWs. The classification is modified from the one used by SW and in the UWWTD.

Classification	**Description**
P (Primary treatment)	Includes works whose treatment methods are restricted to primary treatment (e.g., screening, comminution, maceration, grit and detritus removal, pre-aeration and grease removal, storm tanks, plus primary sedimentation, including where assisted by the addition of chemicals).
SAS (Secondary Activated Sludge)	As primary, plus works whose secondary treatment methods include activated sludge (including diffused air aeration, coarse bubble aeration, mechanical aeration, oxygen injection, submerged filters) and other equivalent techniques.
SB (Secondary Biological)	As primary, plus works whose secondary treatment methods include biological filtration (including trickling filters, conventional filtration, high-rate filtration, double filtration etc.).
TA (Tertiary Activated Sludge)	As SAS, plus tertiary treatment using prolonged settlement in lagoons, constructed wetlands, filters (e.g., sand, nitrifying and/or moving bed filters), nutrient control (using chemical and biological methods), disinfection etc.
TB (Tertiary Biological)	As SB, plus tertiary treatment using prolonged settlement in lagoons, constructed wetlands, filters (e.g., sand, nitrifying and/or moving bed filters), nutrient control (using chemical and biological methods), disinfection etc.

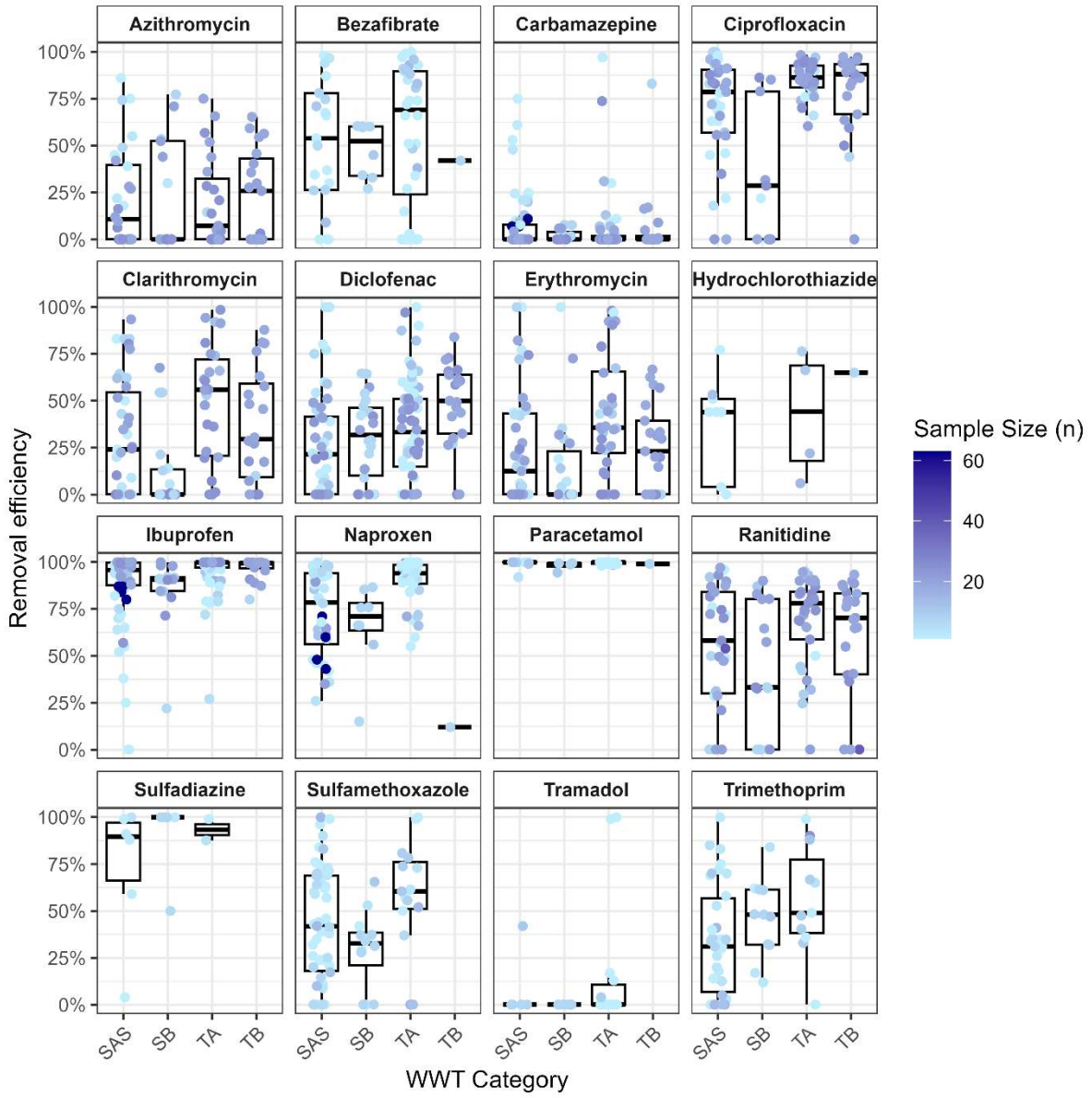

Figure S2.4: Removal efficiencies of the 16 target pharmaceuticals by different treatment categories (see 'Data and code availability').

S2.5 Distance metrics

Table S2.5. Interpretation guidelines for the two distributional comparison metrics used in this study. The interpretation thresholds of W1_log10 have been defined to reflect fold-differences, while the thresholds for JSD are from Acker et al. (2025).

Metric	Threshold	Meaning
Log-Wasserstein distance (W1_log10)	<0.3	Very good agreement (< 2× difference).
	0.3–0.7	Good agreement (≈2–5× difference).
	0.7–1.0	Moderate agreement (≈5–10× difference).
	>1.0	Poor agreement (> 10× difference).
Jensen–Shannon divergence (JSD)	<0.1	Very similar distributions.
	0.1–0.3	Moderate similarity.
	>0.3	Markedly different distributions.

S3. Results

S3.1 Observed pharmaceutical concentrations in Almond River

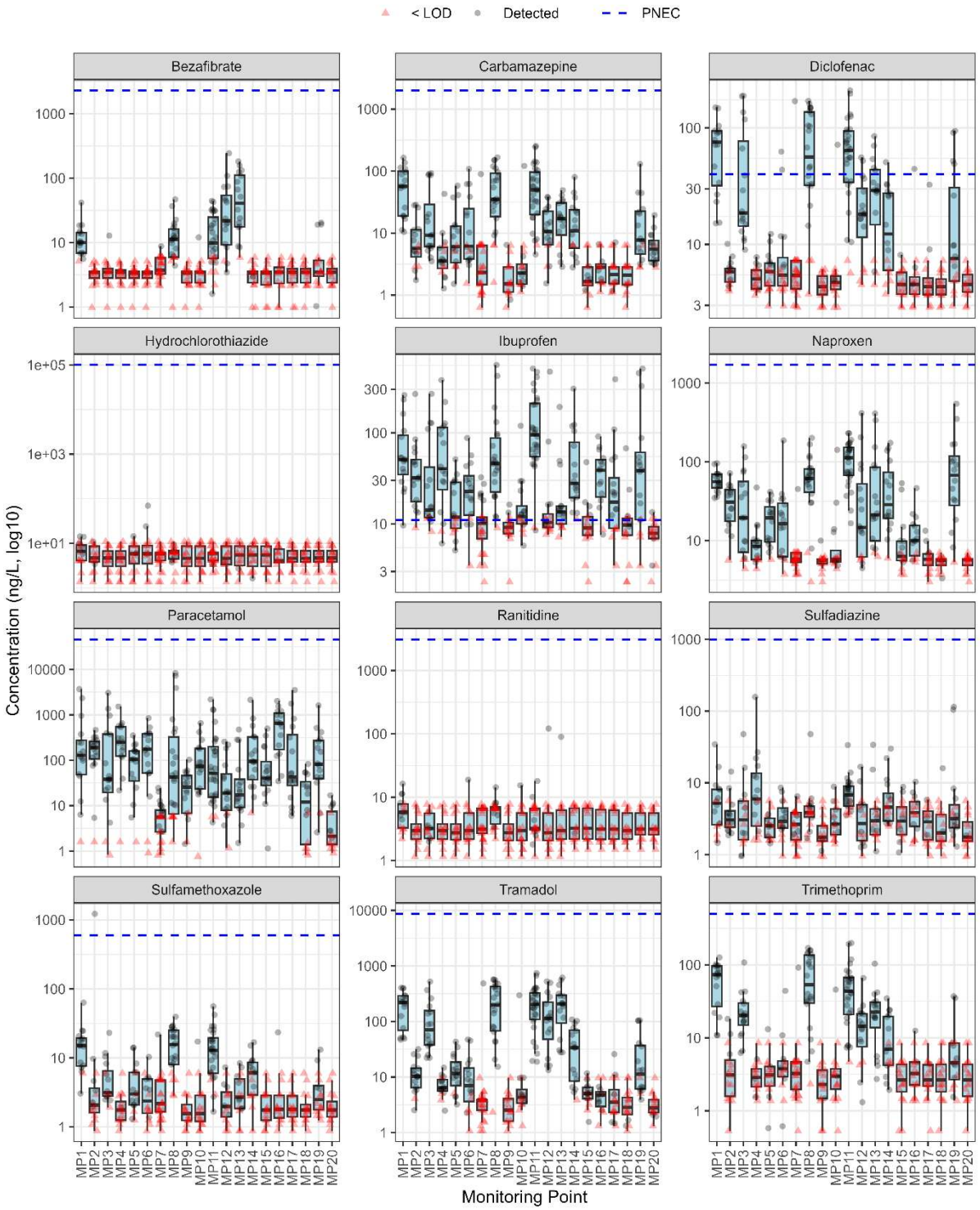

Figure S3.1: Observed concentrations of 12 target compounds at the 20 monitoring points in the Almond catchment (Sept 2023 – Dec 2024). Blue dashed lines show the PNEC value for the respective pharmaceutical.

Table S3.1. Detection frequency (%) of pharmaceutical in the River Almond by monitoring point (MP) during monthly sampling campaign from Sept 2023 to Dec 2024. The STW influence column indicates whether known sewage treatment plants are located within the catchment of the given MP (see Table 2)

MP	STW influence	BZF	CBZ	DFC	HCT	IBU	NAP	PAR	RAN	SDZ	SMX	TML	TMP
1	Yes	94%	100%	100%	38%	100%	100%	94%	50%	69%	94%	100%	100%
2	Yes	0%	75%	56%	13%	94%	94%	94%	0%	81%	38%	94%	19%
3	Yes	6%	100%	100%	0%	81%	81%	88%	31%	56%	75%	100%	100%
4	Yes	0%	69%	25%	0%	94%	69%	94%	0%	69%	6%	81%	19%
5	Yes	0%	75%	38%	13%	63%	94%	94%	0%	38%	75%	94%	25%
6	Yes	0%	81%	38%	19%	88%	81%	88%	6%	63%	44%	69%	44%
7	No	4%	4%	4%	0%	32%	4%	44%	0%	20%	4%	4%	4%
8	Yes	77%	86%	86%	23%	95%	91%	73%	36%	45%	77%	95%	95%
9	No	0%	13%	0%	0%	19%	13%	88%	0%	13%	0%	0%	6%
10	No	6%	44%	19%	0%	69%	50%	94%	6%	38%	6%	44%	13%
11	Yes	75%	96%	93%	14%	96%	100%	93%	25%	82%	89%	100%	96%
12	Yes	94%	88%	75%	6%	44%	81%	88%	6%	56%	31%	100%	88%
13	Yes	94%	94%	81%	6%	75%	88%	100%	6%	44%	50%	100%	100%
14	Yes	6%	88%	63%	6%	94%	94%	94%	6%	56%	56%	94%	75%
15	No	0%	31%	6%	0%	25%	50%	100%	0%	38%	0%	56%	0%
16	No	0%	33%	20%	0%	93%	73%	100%	0%	40%	7%	60%	13%
17	Yes	0%	19%	13%	0%	69%	25%	100%	0%	19%	0%	31%	6%
18	No	0%	6%	0%	0%	31%	13%	63%	0%	13%	0%	13%	0%
19	No	25%	81%	56%	0%	75%	94%	94%	0%	69%	25%	88%	56%
20	No	0%	88%	0%	0%	19%	0%	44%	0%	6%	0%	19%	0%
Total		26%	64%	45%	7%	68%	65%	85%	10%	46%	36%	67%	45%

S3.2 Model performance

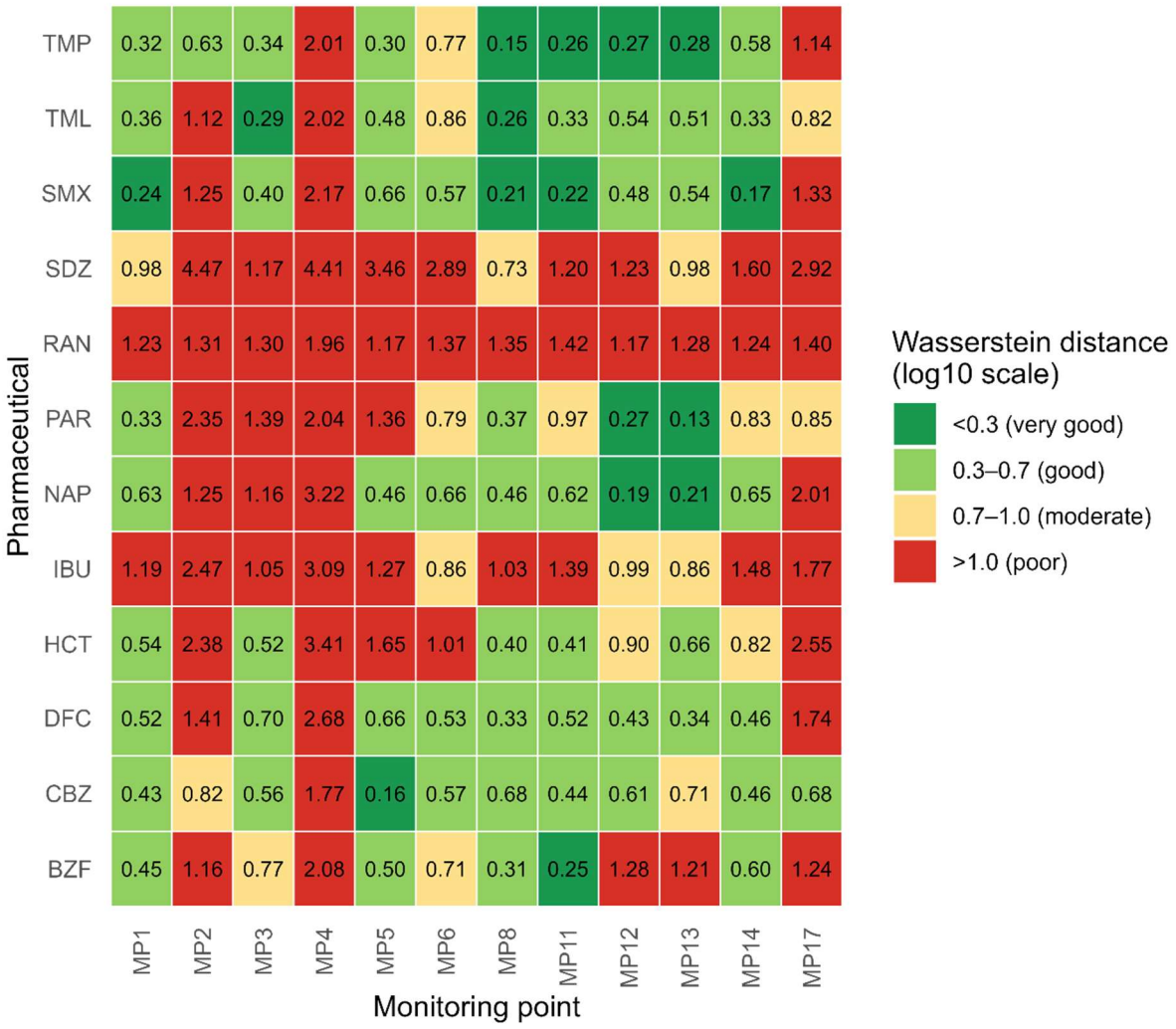

Figure S3.2: Heatmap of calculated log10-Wasserstein distance by monitoring point and pharmaceutical coloured according to the interpretation thresholds given in Table S2.5.

Figure S3.3: Heatmap of calculated JSD distance by monitoring point and pharmaceutical coloured according to the interpretation thresholds given in Table S2.5. At monitoring points (e.g. MP17) where a large proportion of observations are censored, JSD is less sensitive and underestimates discrepancies in distribution shape (see section 3.2).

S3.3 Risk assessment

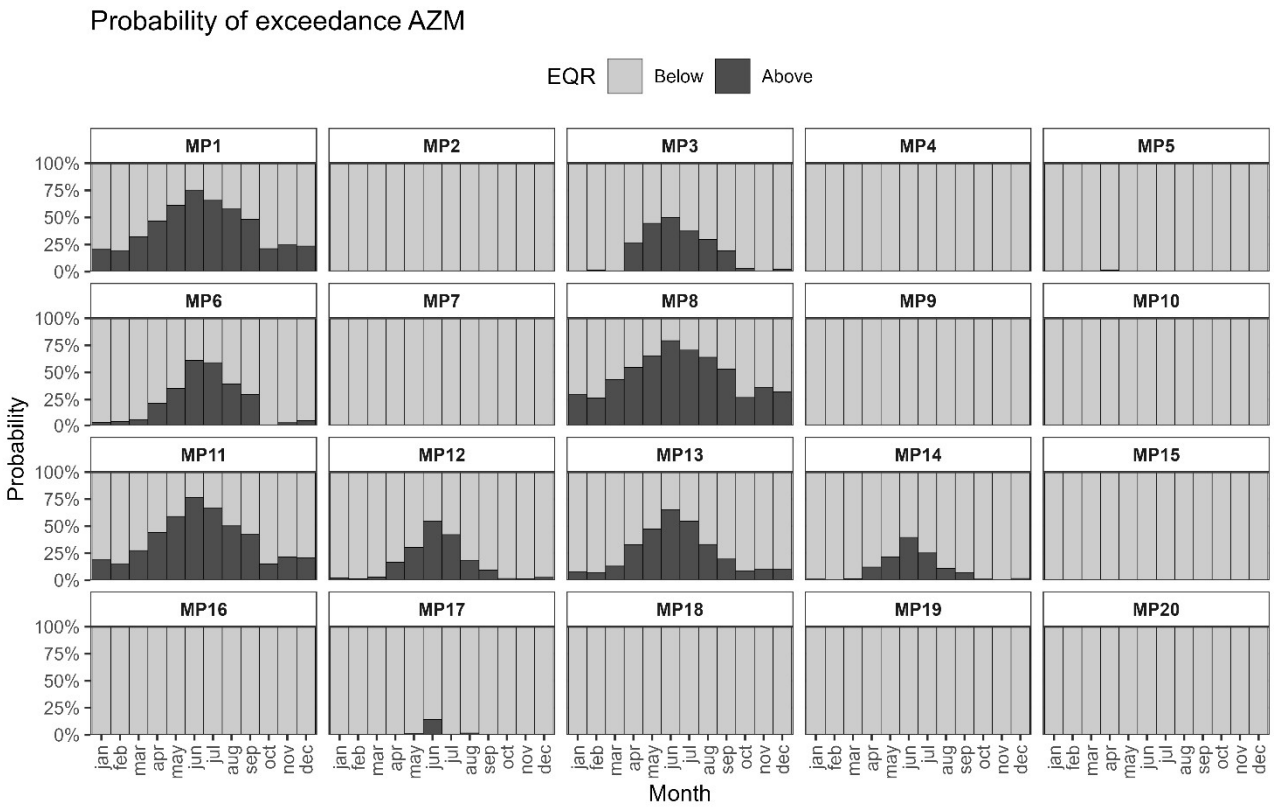

Figure S3.4: Simulated probability of azithromycin (AZM) exceeding the PNEC.

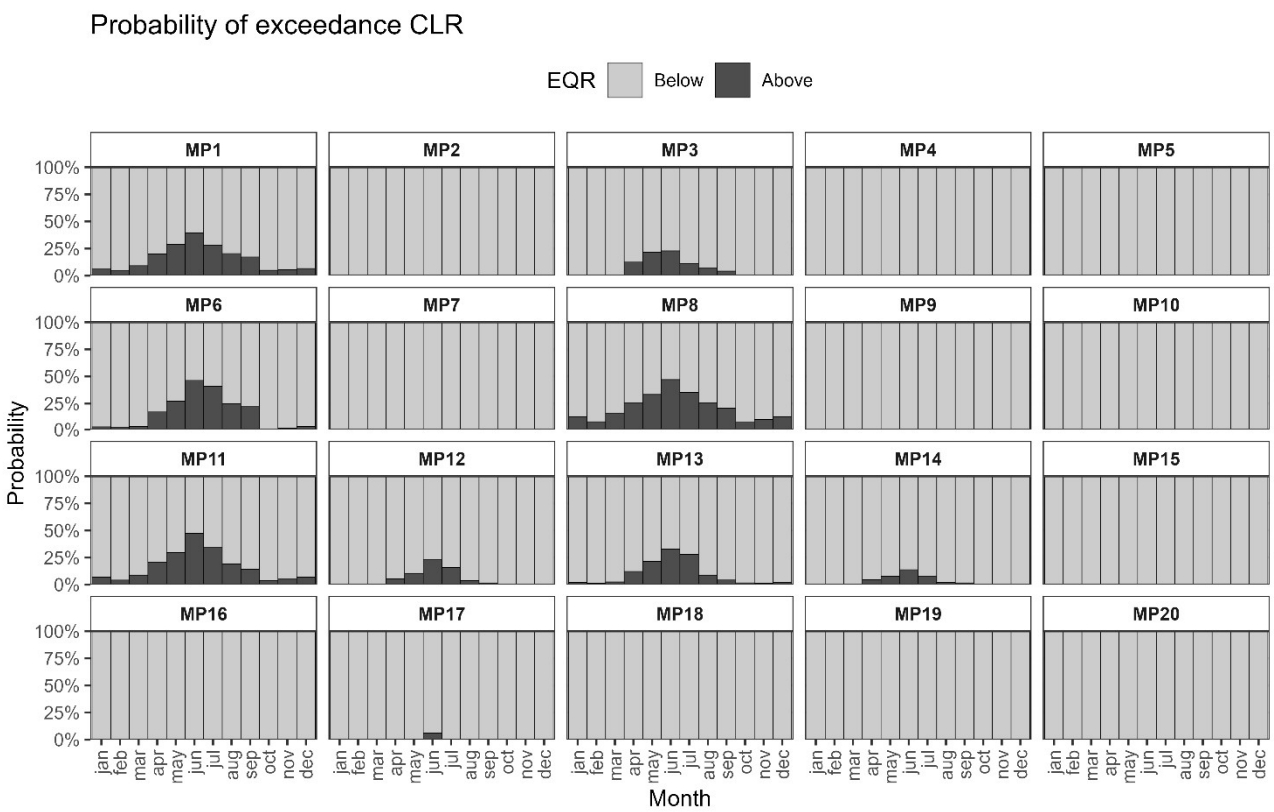

Figure S3.5: Simulated probability of clarithromycin (CLR) exceeding the PNEC.

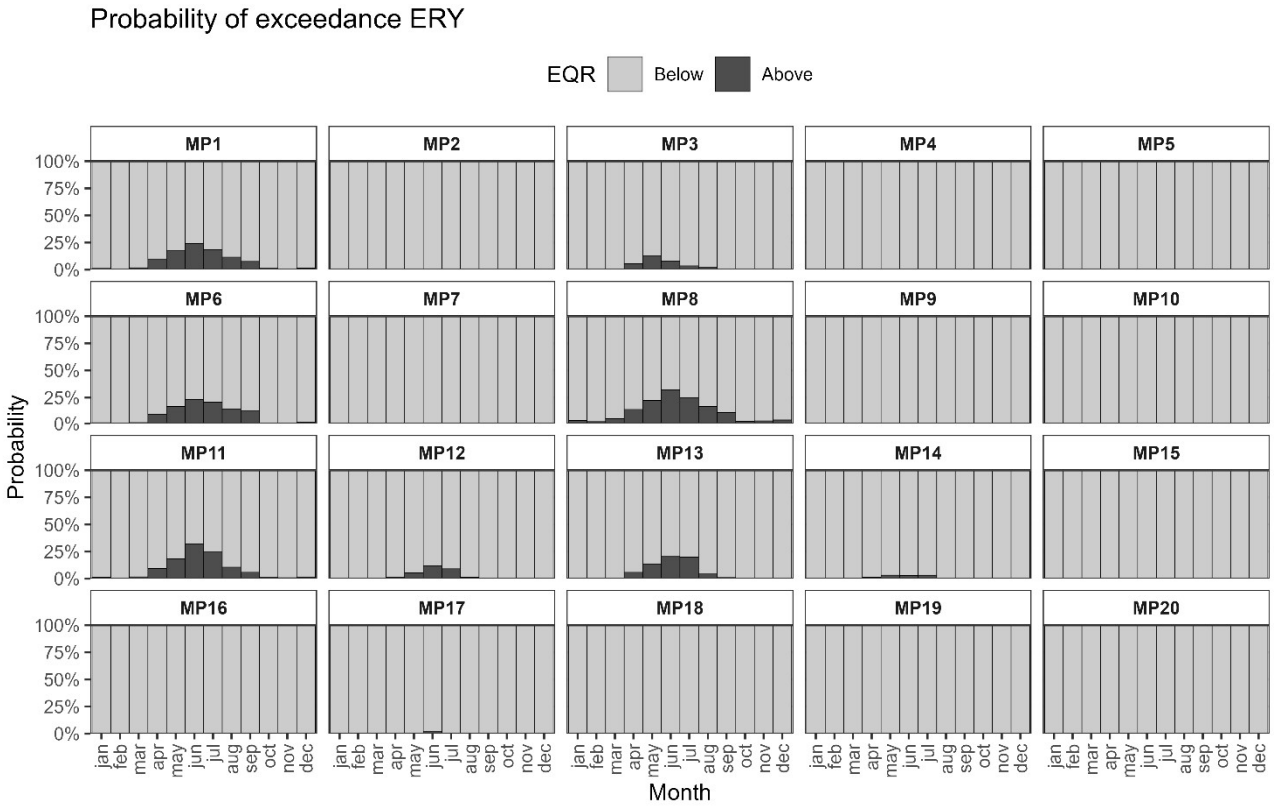

Figure S3.6: Simulated probability of erythromycin (ERY) exceeding the PNEC.

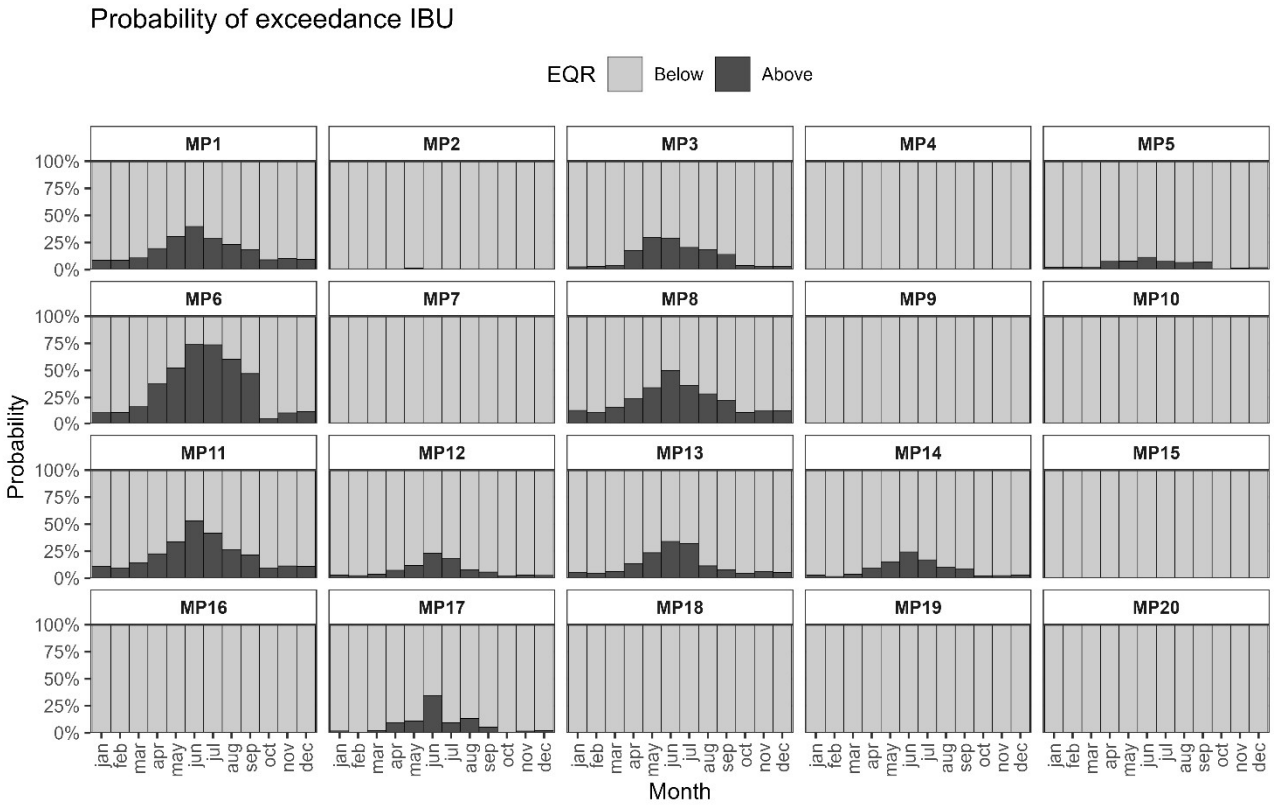

Figure S3.7: Simulated probability of ibuprofen (IBU) exceeding the PNEC.

S3.3 Scenario analysis

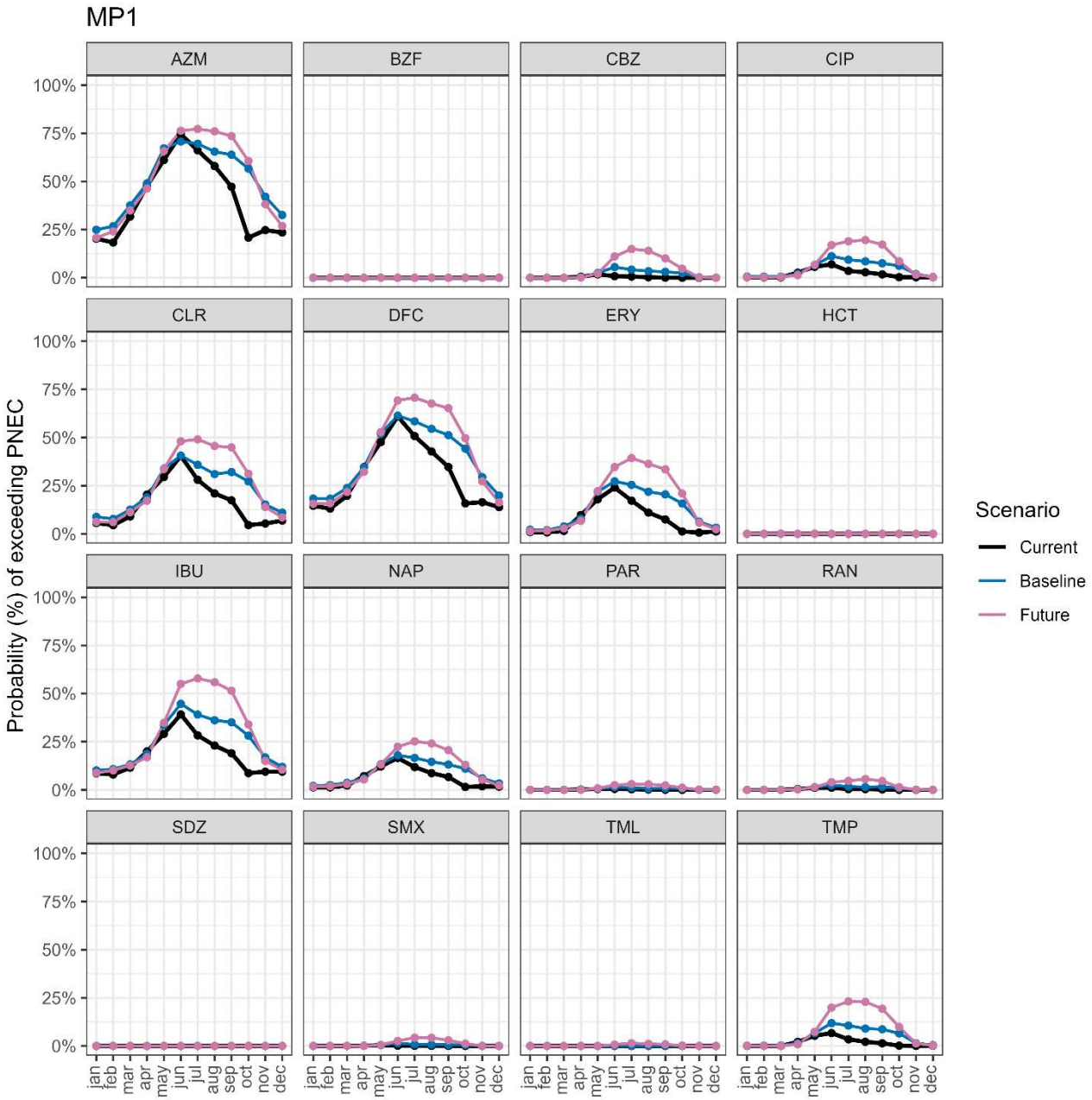

Figure S3.8. Probability of exceeding the PNEC for each of the 16 target pharmaceuticals at location MP1 for the current climate situation and for the baseline (1990-2020) and the future climate (2050-2080) periods.

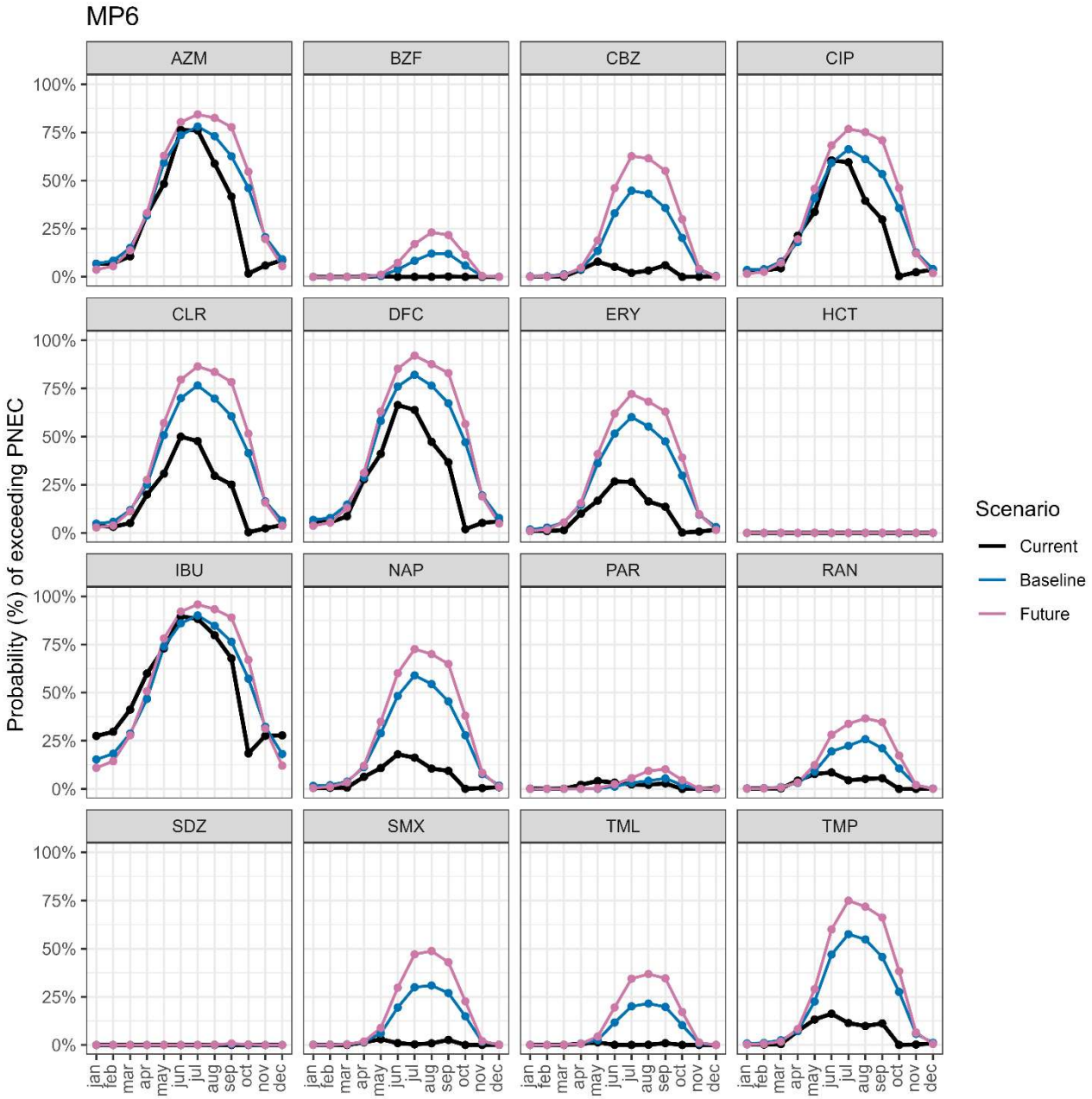

Figure S3.9. Probability of exceeding the PNEC for each of the 16 target pharmaceuticals at location MP6 for the current climate situation and for the baseline (1990-2020) and the future climate (2050-2080) periods.

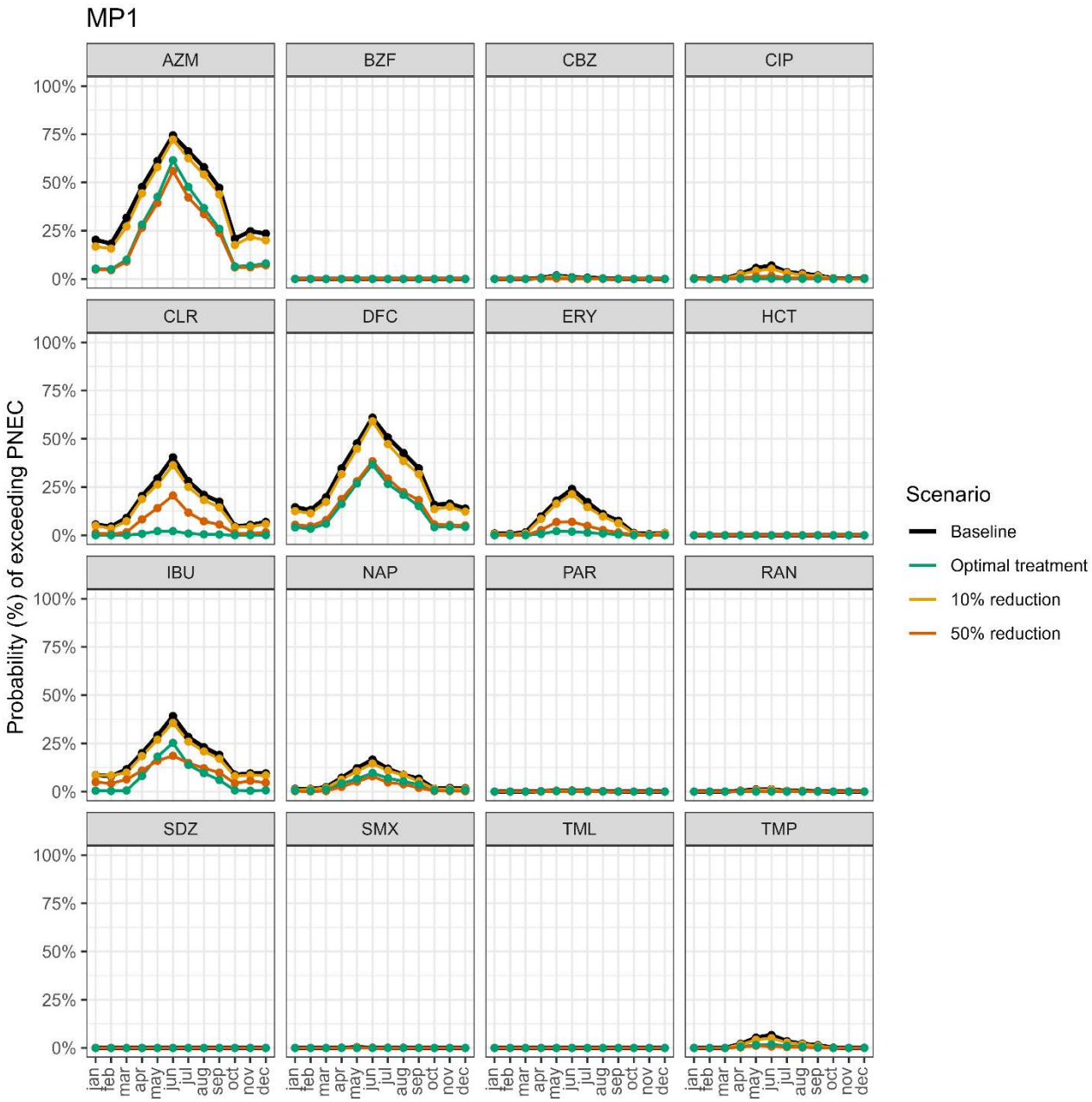

Figure S3.10. Probability of exceeding the PNEC for each of the 16 target pharmaceuticals at location MP1 for the baseline situation and for three different management scenarios: optimal treatment, reduction in prescription rates by 10% and reduction in prescription rate by 50%.